horticulturae

MDPI

Article

Non-Destructive Assessment of Nutrient Status in 'Nashi' Pear Trees Using Optical Methods

Pedro Tomas Bulacio Fischer [1,*], Alessandro Carella [1], Roberto Massenti [1], Sofia Maria Muscarella [1], Andrés Marzal [2] and Riccardo Lo Bianco [1,*]

[1] Department of Agricultural, Food and Forest Sciences (SAAF), University of Palermo, 90128 Palermo, Italy; alessandro.carella@unipa.it (A.C.); roberto.massenti@unipa.it (R.M.); sofiamaria.muscarella@unipa.it (S.M.M.)
[2] Instituto Valenciano de Investigaciones Agrarias, 46113 Moncada, València, Spain; marzal_and@gva.es
* Correspondence: pedrotomas.bulaciofischer@unipa.it (P.T.B.F.); riccardo.lobianco@unipa.it (R.L.B.)

Abstract

Efficient nutrient management is essential for sustainable orchard production; however, conventional laboratory analyses used to assess plant nutritional status are time-consuming and expensive. Optical sensing technologies offer a rapid and non-destructive alternative. This study evaluated the potential of proximal optical sensors and UAV-based multispectral imagery to assess the nutritional status of young potted 'Nashi' pear (*Pyrus pyrifolia* (Burm. f.) Nakai) trees. Three fertilization treatments based on different concentrations of Hoagland solution were applied to 18 one-year-old potted trees. Leaf measurements were collected during the growing season using Dualex, CL-01 chlorophyll meter, and Pocket PEA fluorimeter, while UAV-based multispectral imagery was used to calculate vegetation indices, including NDVI, SR, OSAVI, and MSAVI. Leaf nitrogen (N), phosphorus (P), and potassium (K) concentrations were chemically determined and used as reference values for the regression analyses. Significant ($p < 0.05$) relationships were observed between leaf N content (N%) and several optical parameters related to leaf pigments, including chlorophyll, flavonols, and the Nitrogen Balance Index (NBI), as well as multispectral indices, although with weak associations (R^2 = 0.326–0.488). The strongest individual relationship with N% was shown by NBI (R^2 = 0.480). To account for repeated measurements on the same plants, linear mixed-effects models were fitted. These models indicated that NBI showed the strongest association with N% among the proximal optical parameters (β = 0.019, $p < 0.001$; RMSE = 0.113; MAE = 0.091), followed by flavonols and Dualex chlorophyll. In contrast, optical parameters showed limited sensitivity to P and K. Multispectral indices were not significantly related to K, while only Red and Green reflectance showed weak correlations with P. Overall, optical parameters showed the best associations with N% under the combined nutrient-gradient conditions tested, whereas the assessment of P and K remained limited and should be considered exploratory.

Keywords: chlorophyll; flavonols; fluorescence; remote multispectral sensing; Nitrogen Balance Index; proximal sensing; foliar nutrition

Check for updates

Academic Editor: Daniela Farinelli

Received: 28 May 2026
Revised: 23 June 2026
Accepted: 25 June 2026
Published: 27 June 2026

Copyright: © 2026 by the authors. Licensee MDPI, Basel, Switzerland. This article is an open access article distributed under the terms and conditions of the Creative Commons Attribution (CC BY) license.

1. Introduction

Due to the increasing food demand driven by a growing global population and the scarcity of non-renewable resources, the sustainable management of inputs to minimize waste has become a crucial priority [1,2]. In agriculture, farmers rely on fertilization to enhance crop yield and ensure sufficient production to cover food demand [3]. However,

fertilizer application rates are not always well aligned with plant requirements; indeed, under-fertilization can result in suboptimal yields, whereas excessive application leads to resource waste and may trigger additional problems, such as soil and groundwater contamination [4,5]. Among the nutrients supplied to plants with fertilization, macronutrients such as nitrogen (N), phosphorus (P), and potassium (K) are of primary importance for plant growth and physiological functioning [6].

These essential macronutrients are involved in key physiological and metabolic processes regulating plant growth and productivity [7]. Nitrogen is closely associated with chlorophyll (Chl) synthesis and photosynthetic activity [8], P plays a central role in energy transfer and carbon metabolism [9], while K contributes to osmotic regulation, stomatal functioning, assimilate transport, and stress tolerance [10]. Consequently, deficiencies in these nutrients can alter plant physiological performance and potentially influence optical and spectral responses associated with plant nutritional variability.

Traditionally, plant nutritional status has been assessed in laboratory settings using chemical-analytical techniques such as visible and near-infrared spectroscopy [11], flame atomic absorption spectroscopy [12], mass spectrometry [13], chromatography [14], and fluorescence-based methods [15]. Several of these approaches provide high precision and sensitivity for nutrient determination. However, their practical applicability may differ substantially depending on the technique employed. For example, spectroscopic approaches such as near-infrared spectroscopy can be implemented through portable devices and may require limited sample preparation, whereas techniques such as mass spectrometry, chromatography, and atomic absorption spectroscopy generally rely on expensive and specialized laboratory instrumentation, destructive sampling, technical expertise, and more time-consuming analytical procedures [16]. In recent decades, precision horticulture has emerged as a fundamental approach for orchard management, aiming to optimize the use of inputs and labor while maintaining high productivity and improving overall system sustainability [17]. Within this framework, fertilization plays a central role. Rather than simply supplying nutrients, it focuses on adjusting both the timing and rate of application according to the crop's specific and dynamic requirements, ensuring a balanced and continuous nutrient supply throughout the growing season [18].

Plant nutritional status is influenced by complex physiological and biochemical processes, including nutrient interactions, different chemical forms, metabolic redistribution, and variations associated with phenological stage and plant physiological conditions [6,16,19]. Therefore, developing robust and universally reliable non-destructive techniques for nutrient status assessment remains challenging.

Among the physico-chemical principles explored in precision horticulture for assessing plant nutritional status, optical-based approaches have received particular attention. Optical approaches rely on the physico-chemical principles governing the interaction between electromagnetic radiation and plant tissues, which generate specific spectral responses as a function of the biochemical and structural properties of vegetation [20]. Leaf reflectance and absorbance in the visible and near-infrared regions are primarily influenced by the concentration of photosynthetic pigments, the internal structure of the leaf mesophyll, and the water status of the tissues [21]. Other sensors operate on fluorescence principles, measuring Chl fluorescence emitted by leaf tissues following light excitation [22]. This signal provides insights into the efficiency of the photosynthetic apparatus and can be affected by nutrient availability, since deficiencies may modify electron transport processes, energy dissipation mechanisms, and overall photosynthetic performance [15].

Regarding agricultural remote sensing, multispectral systems represent one of the most widely adopted and well-established tools for crop monitoring [23]. These systems enable the computation of vegetation indices such as the Normalized Difference Vegetation Index

(NDVI), the Enhanced Vegetation Index (EVI), the Green Normalized Difference Vegetation Index (GNDVI), and the Soil Adjusted Vegetation Index (SAVI), derived from reflectance measurements in specific spectral bands [24,25]. However, these indices are generally related to canopy vigor, biomass, and Chl content rather than to a direct quantification of plant nutrient status [26].

As for proximal sensing, several optical leaf-clip sensors have been developed based on reflectance and absorbance measurements in the visible and near-infrared (NIR) regions. Instruments such as Dualex, SPAD-502, and the CL-01 Chlorophyll Meter are designed to estimate leaf-level contents of Chl, flavonols (Flav), and anthocyanins (Anth), providing rapid and non-destructive assessments of plant physiological traits [27,28]. On the other hand, there are handheld instruments known as fluorometers, such as the Pocket PEA, which measure fast Chl fluorescence transients (the OJIP curve) following a brief pulse of high-intensity light applied to dark-adapted leaves [29]. These devices analyze the kinetics of fluorescence emission to assess the functionality and efficiency of photosystem II (PSII), providing information on the integrity of the photosynthetic apparatus, electron transport efficiency, and plant stress conditions [30].

In orchard systems, rapid and non-destructive optical sensing provides a practical alternative to destructive leaf analyses for diagnosing nutritional constraints. In a study conducted in a pear (*Pyrus communis* L.) orchard of the cv. RedBlush, leaf and canopy-level reflectance measurements, acquired using a portable spectrometer and a multispectral camera mounted on an Unmanned Aerial Vehicle (UAV), were used to calculate several vegetation indices that were subsequently compared with laboratory-determined leaf N content. At the leaf level, the most effective indices were NDVI and NDRE (720 nm), achieving R^2 values of 0.65 [31]. Treder et al. [32] developed a non-destructive approach to estimate leaf N content in apple trees (*Malus domestica* Borkh.) based on digital image analysis of scanned leaves. The study compared traditional Chl meters (SPAD-502 and CCM-200) with RGB color component analysis derived from flatbed scanner images and chemically determined N content. While SPAD and CCM showed significant correlations with leaf N, the strongest predictive performance was obtained using multiple regression models based on RGB color components, particularly red and blue values combined with leaf age (R^2 = 0.91). Cerovic et al. [33] developed and validated a nondestructive optical method for diagnosing N status in grapevine (*Vitis vinifera* L.) using the Dualex leaf-clip device under field conditions. The study calibrated Chl, epidermal Flav, and the N Balance Index (NBI = Chl/Flav) against leaf N content determined by Dumas and Kjeldahl analyses across multiple vineyards, cultivars, and phenological stages. Among the tested indices, NBI provided the most robust estimation of leaf N content (RMSE < 2 mg g^{-1} DW at plot level), outperforming Chl alone. The authors proposed threshold values of Chl and NBI for classifying N deficiency, sufficiency, and excess at flowering and bunch closure stages and defined a standardized sampling protocol (36–60 leaves at a fixed node position).

Despite their operational simplicity and non-destructive nature, optical sensors provide indirect proxies of plant nutritional status, being primarily sensitive to Chl-related traits and photosynthetic performance [34]. Their signal can be confounded by canopy structure, phenological stage, water stress, and environmental conditions, limiting nutrient specificity and cross-site transferability of predictive models. To overcome these limitations, the cited authors strongly recommend performing a site- and cultivar-specific calibration, together with careful standardization of leaf position and phenological stage at the time of measurement [34,35]. Most studies available in the literature have focused on the use of both proximal and remote optical sensors for estimating leaf N content, mainly through its correlation with leaf Chl content [35,36]. However, previous studies have generally focused on specific sensing approaches or on selected physiological indicators, mainly

leaf N estimation [37,38]. Information regarding the integrated use of proximal optical sensing, Chl fluorescence measurements, and UAV-derived multispectral vegetation indices within the same experimental framework for the assessment of N, P, and K variability in fruit trees remains limited. Compared with N, whose optical detection is strongly linked to Chl-related traits and photosynthetic proteins [39], the relationships between optical responses and P or K are less direct and less well established. Phosphorus may influence leaf optical properties through its role in photosynthetic pigment synthesis [40], energy metabolism [41], and carbon allocation [42], which can indirectly affect reflectance in the visible range [40,43]; K, in turn, affects stomatal regulation, turgor maintenance, and plant water relations [44]. Alterations in K status may therefore indirectly affect Chl fluorescence parameters and near-infrared reflectance [45]. Therefore, the assessment of P and K in this study should be considered exploratory and aimed at evaluating whether integrated optical measurements can capture broader nutrient-related variability under the experimental conditions tested.

Based on these considerations, this study provides a preliminary comparative evaluation of proximal optical sensing, Chl fluorescence measurements, and UAV-based multispectral imagery for the non-destructive assessment of nutrient variability in young potted 'Nashi' pear (*Pyrus pyrifolia* (Burm. f.) Nakai) trees. The study specifically aimed to compare the relationships between different optical parameters and chemically measured leaf N, P, and K contents and to identify which sensing approaches were most closely associated with nutrient variability under the combined nutrient-gradient conditions tested.

2. Materials and Methods

2.1. Location

The experiment was conducted from May to August 2025 under an outdoor plastic shed located at the Department of Agricultural, Food and Forest Sciences (SAAF), University of Palermo (38.1076° N, 13.3499° E; WGS84). The structure was covered with a polyethylene plastic film transmitting approximately 70% of incoming solar radiation and was open on the sides. For the trial, 18 one-year-old 'Nashi' pear trees grafted onto wild pear (*Pyrus pyraster* (L.) Burgsd) were used (Figure 1A). Therefore, plants were protected from direct rainfall and grown under natural sunlight filtered by the polyethylene cover, without artificial lighting, heating, cooling, or controlled photoperiod conditions. Air temperature, relative humidity, and light intensity recorded during the experimental period are reported in the Supplementary Materials (Figures S1 and S2). Trees were transplanted into 9.5 L pots using sieved and washed river sand (0–1 mm particle size) as the substrate (Figure 1B). Each pot was placed on a load cell sensor (Mitomoi Elettronica di Bravo Maria, Palermo, Italy) to monitor the amount of water lost by evapotranspiration and replace it to maintain soil water around field capacity (Figure 1C).

2.2. Experimental Design

On 8 May 2025, three treatments were applied, each consisting of six replicates: a control group irrigated exclusively with tap water (H0%); a group fertigated with a standard Hoagland Modified Basal Salt Mixture (PhytoTechnology Laboratories™, LLC, Lenexa, KS, USA) [46] diluted to a 1:25 concentration (H4%); and a group fertigated with the same Hoagland solution diluted to 1:5 (H20%). The chemical composition of the Hoagland solution used is reported in Table 1. Based on the nutrient composition of the full-strength Hoagland solution, the estimated concentrations of the main nutrients were 210.2 mg L^{-1} N, 30.9 mg L^{-1} P, and 234.6 mg L^{-1} K. Accordingly, the H4% treatment supplied approximately 8.41 mg L^{-1} N, 1.24 mg L^{-1} P, and 9.38 mg L^{-1} K, whereas the H20% treatment supplied approximately 42.04 mg L^{-1} N, 6.18 mg L^{-1} P, and 46.92 mg L^{-1} K.

These values represent nominal nutrient concentrations in the irrigation solution rather than actual nutrient uptake or cumulative nutrient input per plant. Because irrigation was managed, as specified before, to maintain soil water around field capacity, the volume applied to each plant varied according to plant loss through evapotranspiration. To prevent salt accumulation in the pots, which could negatively affect tree growth, all trees in trial were irrigated with abundant tap water every 15 days to leach any excess of salts. After each leaching irrigation, the treatment-specific fertigation regime was resumed, and trees continued to receive water or nutrient solutions according to their assigned treatments. The different Hoagland concentrations generated a combined nutrient gradient. Therefore, the experimental design was intended to induce overall nutrient variability among trees, but it did not allow the independent isolation of the effect of each nutrient. However, the relationships between optical measurements and nutrient status were evaluated using chemically determined leaf N, P, and K concentrations obtained from laboratory analyses, rather than the nominal nutrient concentrations in the irrigation solutions.

Figure 1. Layout of the pots used in the experiment (**A**), tree potting using sand as substrate (**B**) and load cells used to monitor water loss (**C**).

Table 1. Chemical composition of the Hoagland solution used during the trial.

Chemicals	mg L^{-1}
Ammonium Phosphate, Monobasic	115.0
Boric Acid	2.9
Calcium Nitrate	656.4
Cupric Sulphate·5H_2O	0.1
Na_2EDTA·2H_2O	3.4
Ferrous Sulphate·7H_2O	2.5
Magnesium Sulphate, Anhydrous	240.8
Manganese Chloride·4H_2O	1.8
Molybdenum Trioxide	0.0
Potassium Nitrate	606.6
Zinc Sulphate·7H_2O	0.2

2.3. Optical Instrument Measurements

During the experiment, weekly non-destructive optical measurements were carried out on each plant using the Pocket PEA (Hansatech Instruments Ltd., King's Lynn, Norfolk, UK) (Figure 2A), Dualex Scientific+ (Force-A, Orsay, France) (Figure 2B), and CL-01 Chlorophyll Meter (Hansatech Instruments Ltd., King's Lynn, Norfolk, UK) (Figure 2C). Before each measurement session, all proximal instruments were started and checked according to the manufacturer's instructions, including standard blank or reference readings where required. For each plant and sampling date, two fully expanded, visually healthy leaves located in the central portion of current-season shoots were selected. For Pocket PEA measurements, one fluorescence transient was recorded on each of the two selected leaves after 20 min of dark adaptation, and the two measurements were averaged to obtain one representative value per plant and sampling date. For Dualex and CL-01 measurements, two readings were taken on each of the two selected leaves, resulting in four readings per plant, which were averaged to obtain one plant-level value for each sampling date.

The Pocket PEA is a portable fluorimeter based on the recording of the OJIP kinetic curve using saturating light pulses under dark-adapted conditions; it provides parameters related to PSII photochemical efficiency and electron transport functionality in the light reactions of photosynthesis. Before each measurement, leaves were dark-adapted for 20 min using leaf clips to ensure full opening of PSII reaction centers. The device emits a high-intensity red saturating pulse (peak = 650 nm; max. intensity = 3500 µmol m^{-2} s^{-1}), which induces the complete closure of PSII reaction centers and allows the recording of the OJIP curve. From the fluorescence transient, the instrument automatically extracts initial fluorescence (F_0), maximum fluorescence (F_m), and variable fluorescence ($F_v = F_m - F_0$) and calculates the maximum quantum efficiency of PSII photochemistry (F_v/F_m).

The Dualex is an optical device that measures Chl content, epidermal Flav and Anth through a dual-excitation optical principle combining Red/NIR transmittance and UV-induced Chl fluorescence and calculates the NBI, a physiological index that provides an indirect estimate of the plant's N nutritional status. The NBI is calculated as the ratio between Chl and Flav contents; since Chl is positively correlated with N availability, whereas Flav increase under N deficiency, high NBI values indicate a good N nutritional status. Another instrument used was the CL-01 Chlorophyll Meter, a non-destructive device based on dual-wavelength transmittance (660 nm and 960 nm) for estimating Chl content.

Finally, a DJI Mavic 3M drone (DJI, Shenzhen, China) (Figure 2D) equipped with a multispectral camera was used. Specifically, the system includes one RGB camera with a 4/3″ CMOS sensor (20 MP) and four monochrome multispectral sensors (5 MP, 1/2.8″ CMOS) with band centers in Green (G, 560 ± 16 nm), Red (R, 650 ± 16 nm), Red Edge (RE, 730 ± 16 nm), and NIR (860 ± 26 nm).

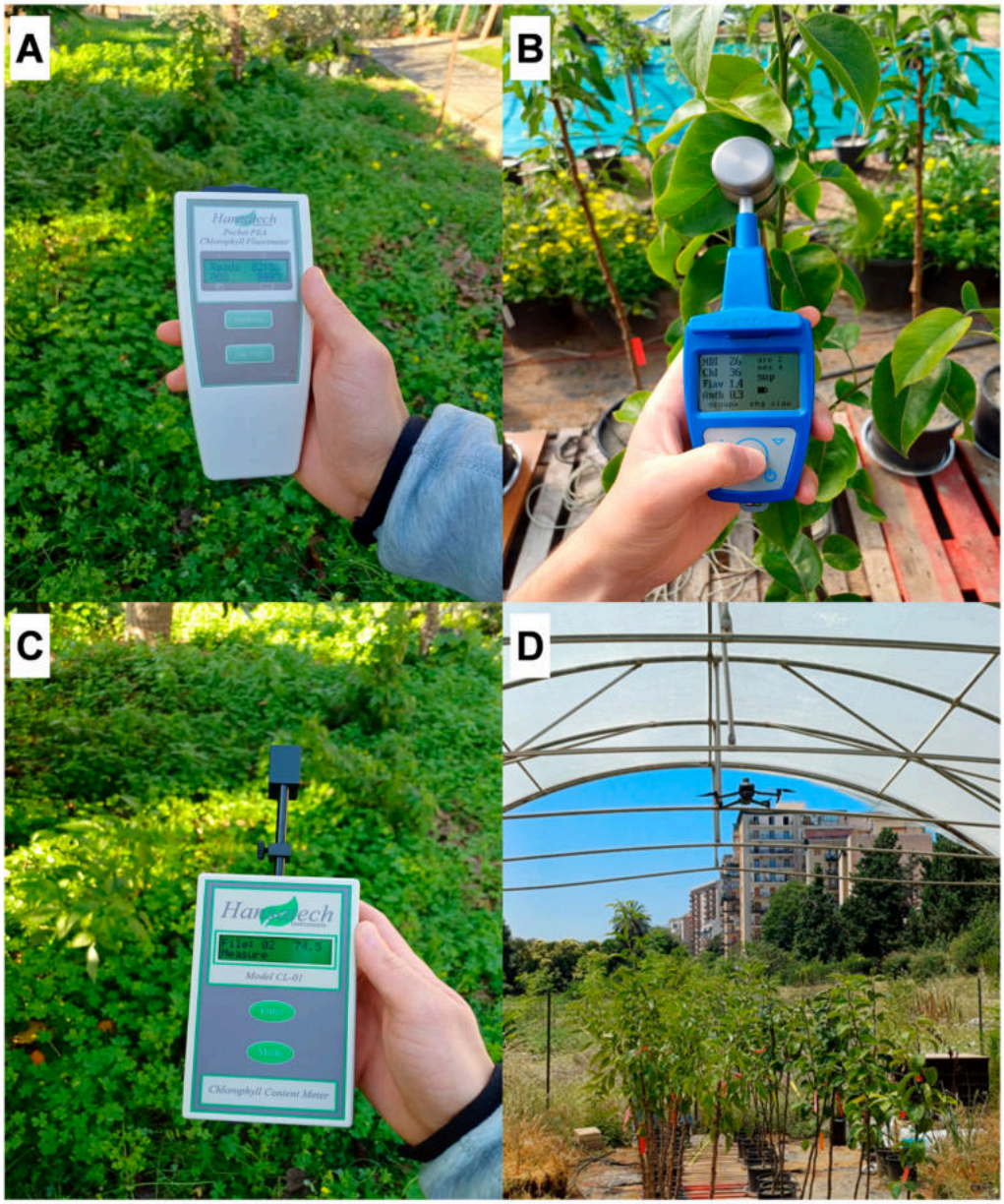

Figure 2. Non-destructive instruments used during the trial, namely the Pocket PEA (**A**), the Dualex (**B**), the Chlorophyll Meter CL-01 (**C**), and the DJI Mavic 3M drone (**D**).

The selected leaves for measurement were representative of the same canopy zone used for subsequent destructive sampling. Therefore, proximal optical measurements and chemical analyses were matched at the plant and canopy-zone level rather than always at the exact individual-leaf level.

2.4. Multispectral Image Analysis

Multispectral images were processed to extract leaf-level spectral information through a multi-step workflow. Raw multispectral images were imported into Agisoft Metashape Professional (version 2.2.1; Agisoft LLC, St. Petersburg, Russia). Radiometric calibration was applied using the onboard sunlight sensor to correct for illumination variability during image acquisition. Subsequently, images were aligned to ensure spatial correspondence among bands. Multispectral images were then generated using the Convert Images tool with the "Merge multispectral images" option enabled, producing band-aligned multispectral images for each acquisition.

The resulting images were imported into QGIS (version 3.40.8; QGIS Development Team) for visualization and preprocessing. In this step, the Normalized Difference Vegetation Index (NDVI) was computed to enhance the contrast between vegetation and background, supporting the subsequent segmentation process. Object-based image segmentation was performed using SAGA GIS v. 9.8.1 (System for Automated Geoscientific Analysis, SAGA User Group Association, Gottingen, Germany; [47]), applying a cluster segmentation approach with three classes, corresponding to background, shadow, and plant.

A manual refinement step was applied to remove non-leaf elements (e.g., stems), ensuring that only leaf pixels were retained for analysis.

Finally, zonal statistics were computed in QGIS to extract spectral information from each leaf. For each object and spectral band (Green, Red, Red Edge, and NIR), descriptive statistics (mean, median, standard deviation, minimum, and maximum) were calculated. The median value was selected as a robust estimator at the leaf level to minimize the influence of mixed pixels and edge effects. For each plant, a single spectral value per band was obtained by averaging the median values across all segmented leaves. Accordingly, UAV-derived multispectral information was considered at the plant level rather than at the individual-leaf level. The resulting plant-level spectral values and vegetation indices were matched with the corresponding leaf-level chemical nutrient analyses.

The extracted spectral bands of each plant were used for the calculation of different vegetation indices (Table 2). To evaluate overall canopy vigor and Chl-related variability, NDVI and GNDVI were used, with GNDVI offering enhanced sensitivity to moderate variations in Chl content. The PSRI was included as an indicator of pigment degradation and senescence processes, allowing the detection of early physiological stress. The NDRE was also calculated using the NIR and Red Edge bands to exploit the sensitivity of the Red Edge region to Chl-related variability. The CI_RE was calculated to estimate Chl content and, indirectly, N status, as its formulation is particularly sensitive to changes in the Red Edge region. To minimize the influence of soil background on the spectral signal, improving the estimation of vegetation vigor under conditions of partial canopy cover OSAVI was included. The TCARI was calculated as an index specifically designed to estimate Chl content while reducing the effects of canopy structure and background reflectance. The MCARI was used as an index specifically designed to quantify Chl absorption while reducing the interference of non-photosynthetic elements, providing a more robust estimation of leaf Chl content. Its improved formulation, MCARI2, was also calculated to further minimize the effects of canopy structure and soil background, enhancing the sensitivity to Chl variations, particularly in dense canopies. The SR was included as a traditional vegetation index based on the ratio between NIR and Red reflectance, known for its sensitivity to biomass and canopy density, although potentially affected by saturation under high vegetation cover. The MSAVI was used to further reduce soil background effects, especially under conditions of sparse vegetation, improving the reliability of vegetation signal extraction in heterogeneous canopies. The MRETVI was calculated as a modified index derived from the triangular vegetation index family, incorporating spectral information from the Green, Red, and NIR regions to improve sensitivity to Chl content and canopy structure. Finally, CCCI was included to estimate Chl content and N status by combining NDVI and NDRE information, thereby reducing saturation effects and improving sensitivity across a wide range of canopy conditions.

Table 2. Vegetation indices calculated to estimate tree nutrient status.

Vegetation Index	Acronym	Equation	Reference
Normalized Difference Vegetation Index	NDVI	$NDVI = \frac{NIR-Red}{NIR+Red}$	[24]
Green Normalized Difference Vegetation Index	GNDVI	$GNDVI = \frac{NIR-Green}{NIR+Green}$	[48]
Plant Senescence Reflectance Index	PSRI	$PSRI = \frac{Red-Green}{NIR}$	[49]
Chlorophyll Index Red Edge	CI_RE	$CI_RE = \frac{NIR}{RedEdge} - 1$	[50]
Transformed Chlorophyll Absorption in Reflectance Index	TCARI	$TCARI = 3 \times [(Red\ Edge - Red) - 0.2 \times (Red\ Edge - Green) \times (Red\ Edge/Red)]$	[51]
Optimized Soil Adjusted Vegetation Index	OSAVI	$OSAVI = \frac{1.16 \times (NIR-Red)}{(NIR+Red+0.16)}$	[52]
Modified Chlorophyll Absorption in Reflectance Index	MCARI	$MCARI = [(Red\ Edge - Red) - 0.2 \times (Red\ Edge - Green)] \times (Red\ Edge/Red)$	[53]
Modified Chlorophyll Absorption Ratio Index 2	MCARI2	$MCARI2 = [1.5 \times (2.5 \times (NIR - Red) - 1.3 \times (NIR - Green))]/\sqrt{[(2 \times NIR + 1)^2 - (6 \times NIR - 5 \times \sqrt{Red}) - 0.5]}$	[54]
Simple Ratio	SR	$SR = \frac{NIR}{Red}$	[55]
Modified Soil Adjusted Vegetation Index	MSAVI	$MSAVI = [2 \times NIR + 1 - \sqrt{((2 \times NIR + 1)^2 - 8 \times (NIR - Red))}]/2$	[56]
Modified Red Edge Transformed Vegetation Index	MRETVI	$MRETVI = 1.2 \times [1.2 \times (NIR - Red) - 2.5 \times (Red\ Edge - Red)]$	[51]
Normalized Difference Red Edge Index	NDRE	$NDRE = \frac{(NIR-Red\ Edge)}{(NIR+Red\ Edge)}$	[57]
Canopy Chlorophyll Content Index	CCCI	$CCCI = \frac{NDRE}{NDVI}$	[58]

2.5. Nutrient Chemical Analyses

To validate the data collected with non-destructive instruments, four leaf samplings were performed on 8 May, 6 June, 31 July, and 29 August 2025 for chemical analysis. The sampled leaves were oven-dried at 65 °C for 48 h and finely ground for subsequent lab analyses. Nitrogen content was determined using the Dumas combustion method [59] with an elemental analyzer (DuMaster D-480, Büchi Labortechnik, Flawil, Switzerland). To determine P and K in leaves, 0.25 g of dried sample was weighed into a porcelain crucible and placed in a muffle furnace at 550 °C for 8 h. After calcination, the ashes were recovered by acid digestion using 10 mL of 2% HNO_3. The resulting solutions were made up to a volume of 10 mL with Milli-Q water and subsequently diluted 1:10 before analysis. Potassium leaf content was determined by Microwave Plasma Atomic Emission Spectroscopy (MP-AES; Agilent 4210 MP-AES, Milan, Italy). Phosphorus leaf content was determined colorimetrically according to the Murphy and Riley [60] method, with absorbance measured at 882 nm using a spectrophotometer (UVmini-1240, Shimadzu Italia srl, Milan, Italy).

2.6. Data Analysis

The data obtained from the measurements collected with the different instruments were analyzed using statistical Python libraries (version 3.13, Python Software Foundation, Wilmington, DE, USA). Specifically, Scikit-learn (version 1.24.1) [61] and Statsmodels (version 0.14.6) [62] libraries were used. Matplotlib (version 3.10.8) [63] library was used to generate plots. In addition, Jamovi software (version 2.6.0, Sydney, Australia) [64] was used to perform the general linear model (GLM) analysis of leaf nutrient content over time, and SigmaPlot software (Systat Software, Inc., San Jose, CA, USA) was used to generate the corresponding GLM plots. The GLM was performed considering sampling date as the within-subject factor, Hoagland treatment as the between-subject factor, and individual plant as the experimental unit repeatedly measured over time. The model tested the main

effects of sampling date and treatment, as well as their interaction. When significant effects were detected, mean separation was performed using Tukey's honestly significant difference (HSD) post hoc test at $p < 0.05$.

Regression procedures were applied with an approach focused on linear and multiple linear relationships between the parameters measured with the instruments and the chemically determined leaf N, P, and K concentrations obtained from laboratory analyses. The multiple linear regression analysis was conducted performing a Backward Elimination procedure based on a significance threshold (p-value < 0.05), which consists of selecting the significant variables from an initial set of predictors. In our case, the initial pool of variables included leaf Chl index, Anth, Flav, and NBI measured with the Dualex; Fv/Fm measured with the Pocket PEA; and Chl index measured with the CL-01 device. Once the Backward Elimination process was completed, a multiple linear regression using the Ordinary Least Squares method was performed, with N% as the dependent variable and the predictors selected through the Backward Elimination approach as the independent variables.

Because repeated measurements were collected from the same plants over time, linear mixed-effects models were subsequently fitted for the proximal optical parameters to account for the non-independence of observations. For each nutrient, separate models were fitted using leaf N, P, or K concentration as the dependent variable. Optical parameters were included individually as fixed-effect predictors, sampling date was included as a fixed effect to account for temporal variation in nutrient concentration, and plant identity was included as a random intercept to account for repeated measurements on the same plants. Models were fitted using maximum likelihood estimation. Optical predictors were kept in their original units to allow direct interpretation of the regression coefficients. Therefore, β coefficients indicate the expected change in nutrient concentration associated with a one-unit increase in the corresponding optical parameter, after accounting for sampling date and repeated measurements on the same plant. Model performance was evaluated using root mean square error (RMSE) and mean absolute error (MAE) calculated from fitted versus observed values.

A multiple linear regression analysis between vegetation indices obtained from UAV image analyses and the results of laboratory measurements was also performed. In this case, the initial set of predictors included the vegetation indices calculated from multispectral data, and the Backward Elimination procedure was used to select the significant variables. In addition, the same approach was applied by combining the parameters measured with proximal sensing instruments and the vegetation indices. In this case, the analysis was conducted by limiting the observations to those collected on the same dates, to ensure that all variables included in the model were measured simultaneously.

3. Results and Discussion

3.1. Nitrogen (N)

Overall, the three Hoagland treatments induced similar N% changes over time, characterized by relatively high values (1.9–2.2%) early in the growing season, followed by a marked decline during the summer period, with values between 1.5 and 1.9% (Figure 3). As expected, the H20% treatment induced the highest N% levels throughout the monitoring period, whereas H0% and H4% showed comparably lower levels (Figure 3).

The decrease in leaf N content observed in June–July, followed by a tendency to increase in August, is typical of young plants undergoing rapid vegetative growth, as reported by Wu et al. [65] on two-year-old *Pyrus bretschneideri* Rehd cv. Huangguan trees. As observed in *Pyrus betulifolia* Bunge [60] and in 'Niitaka' pear [66], during this stage, the expansion of leaf area and the increase in shoot biomass occur more rapidly than the net

accumulation of N, leading to a reduction in its concentration within the tissues, even when N availability in the substrate remains constant.

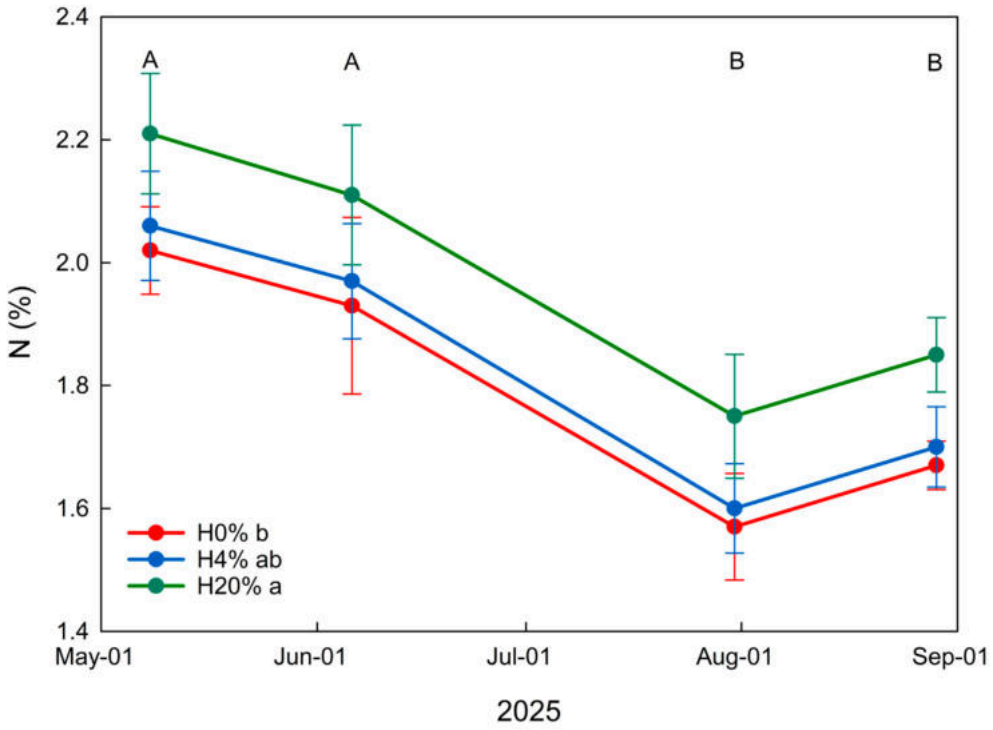

Figure 3. Leaf N content (N, %) determined by chemical analysis in 'Nashi' pear leaves under the three Hoagland solution treatments (H0%, H4%, and H20%) during the trial period. Error bars represent the standard errors of the means. Capital letters on top indicate differences among sampling dates, while lowercase letters in the legend indicate differences among treatments (Tukey's HSD test, $p < 0.05$).

This marked temporal variation in N% supported the inclusion of sampling date as a fixed effect in the subsequent mixed-effects models. Therefore, to account for both temporal variation and repeated measurements on the same plants, the relationships between proximal optical parameters and N% were further evaluated using linear mixed-effects models (Table 3).

Table 3. Linear mixed-effects model results for the relationships between proximal optical parameters (Chl: Chl measured with Dualex; Flav: flavonols measured with Dualex; Anth: anthocyanin measured with Dualex; NBI: Nitrogen Balance Index measured with Dualex; Fv/Fm: maximum quantum efficiency of photosystem II measured with Pocket PEA; CL-01: Chl measured with CL-01 Chlorophyll Meter; CL-01 Filtered: Chl measured with CL-01 Chlorophyll Meter in the last two sampling dates) and leaf nitrogen content (N, %). For each optical predictor, β indicates the slope of each optical predictor, SE the standard error, RMSE the root mean square error, and MAE the mean absolute error.

Predictor	β	SE	*p*-Value	RMSE	MAE
Chl	0.013	0.006	0.033	0.159	0.127
Flav	−0.378	0.142	0.008	0.129	0.104
Anth	−0.935	0.565	0.098	0.149	0.117
NBI	0.019	0.004	<0.001	0.113	0.091
Fv/Fm	−0.058	0.510	0.909	0.149	0.117
CL-01	0.010	0.008	0.180	0.164	0.134
CL-01 Filtered	0.023	0.006	<0.001	0.096	0.076

The mixed-effects analysis was used as a robustness check to evaluate which relationships observed in the simple linear regressions remained significant after accounting for repeated measurements and temporal variability. Overall, the mixed-effects models partially confirmed the results of the linear regressions (Table 3). Among the tested proximal optical parameters, NBI retained a significant positive association with leaf N content ($p < 0.001$) and showed relatively low model-fit errors within the present dataset. The CL-01 Filtered parameter also showed a significant positive association with N% ($p < 0.001$) and provided the lowest prediction errors among the tested, suggesting a slightly better performance in terms of model accuracy. However, these error metrics should be interpreted as descriptive measures of model fit rather than as evidence of validated predictive accuracy. Flav also maintained a significant negative association with leaf N content ($p = 0.008$), while Dualex Chl showed a weaker but still significant positive association ($p = 0.033$). In contrast, Anth, Fv/Fm, and the unfiltered CL-01 parameter were not significantly associated with N% in the mixed-effects framework. Only the linear relationships that were retained as significant in the mixed-effects framework are reported and discussed below.

3.1.1. Dualex

The relationship between Chl content measured with the Dualex and N%, ranging from 1.3 to 2.5%, was linear and direct (Figure 4A), meaning that higher N levels corresponded to higher Chl content. However, the low coefficient of determination ($R^2 = 0.104$) indicated high data variability around the fitted linear trend. Therefore, Chl content alone provided only a weak relationship with N% when all sampling dates were considered, suggesting that additional sources of variability affected the Chl–N relationship. As a result, estimating N% based solely on Chl content appears unreliable, suggesting that a substantial portion of the observed variability is not explained by the regression model (Figure 4A). After restricting the regression analysis to the last two sampling dates (31 July and 29 August), the linear relationship between N% and Chl content measured with the Dualex improves, with a higher coefficient of determination ($R^2 = 0.384$) (Figure 4B).

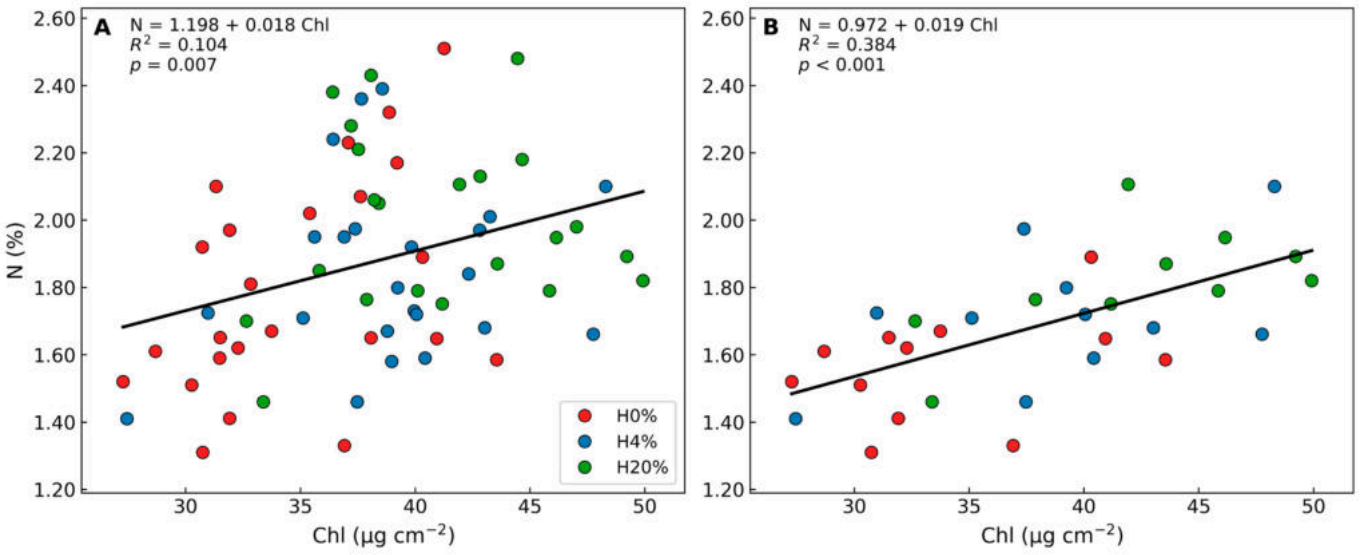

Figure 4. Relationship between leaf Chl content measured with the Dualex device (Chl) and leaf N content (N, %) determined through chemical analysis in 'Nashi' pear, using data from all sampling dates (**A**) or using only the data collected between 31 July and 29 August (**B**). Each point represents an individual plant, with colors indicating different Hoagland treatments (H0%, H4%, and H20%).

The presence of a positive relationship accompanied by high data dispersion is consistent with several studies that used the Dualex device [67,68]. In fruit trees, the Chl index measured with Dualex generally increases with rising N content, in agreement with the physiological role of N in the synthesis of photosynthetic pigments [69]. However, Dualex field applications have shown that the quantitative relationship between Chl content and N% can display high variability and moderate to low coefficients of determination for simple linear models. Such variability has been attributed to physiological factors (leaf age, developmental stage, canopy position, N remobilization within tissues) and environmental conditions (light intensity, water status) [33]. Overall, these studies indicate that Chl content measured with Dualex is a sensitive indicator of N nutritional status, but not always sufficiently robust for an accurate quantitative estimation of N% when used as a single predictor [70].

During the first two sampling dates (8 May and 6 June), the leaves were still expanding and had not yet reached physiological maturity. Moreover, in potted plants, N availability in the substrate can fluctuate rapidly due to environmental factors [71], introducing additional variability in Chl content regardless of the imposed nutrient level. By excluding the first two sampling dates, the analysis focuses on physiologically mature and more stable leaves (Figure 4B), and Chl content more reliably reflects N availability [72]. Under these conditions, the linear model reveals a clear positive relationship fully consistent with the physiological role of N in Chl and photosynthetic protein biosynthesis. Overall, the comparison between the two graphs indicates that optical Chl measurements can reliably estimate N status only when leaves are at a physiologically mature stage, whereas during early or transitional phases the relationship is weakened by growth-related processes [73].

This interpretation was further supported by the linear mixed-effects model, which confirmed a weak but significant positive association between Dualex Chl and N% after accounting for sampling date and repeated measurements on the same plants (Table 3).

The relationship between Anth content measured with the Dualex and N% was negative but weak in the simple linear regression, with Anth explaining only 15.3% of the variability in leaf N content ($R^2 = 0.153$; $p < 0.001$). Although anthocyanin accumulation has been reported to increase under reduced N availability, mainly as part of stress-related and photoprotective responses [74,75], this relationship was not confirmed in the mixed-effects framework (Table 3). Therefore, Anth should be interpreted as a weak and non-robust indicator of leaf N content under the present experimental conditions.

The relationship between Flav content measured with the Dualex and N% was also linear but indirect (Figure 5), showing a decrease in N with increasing Flav content. Although the regression was statistically significant, the coefficient of determination ($R^2 = 0.426$) indicated that a relevant portion of the variability in N% remained unexplained when Flav was used alone. Specifically, the regression model suggests a 57.4% unexplained variability in the prediction of N% when using Flav index alone (Figure 5).

A similar pattern has been reported in the literature for optical measurements obtained with the Dualex, which have shown inverse relationships between Flav content and N%, with higher Flav accumulation under reduced N availability [76]. In maize, the accumulation of optically measured polyphenols and Flav has been closely linked to the leaf carbon–N balance, highlighting a sensitive Flav response to N status [77]. This behavior is consistent with the fact that limited N availability reduces protein synthesis and vegetative growth, altering the carbon–N balance and promoting the reallocation of carbon toward carbon-rich secondary metabolites such as Flav, as demonstrated in physiological validation studies of the Dualex device [78].

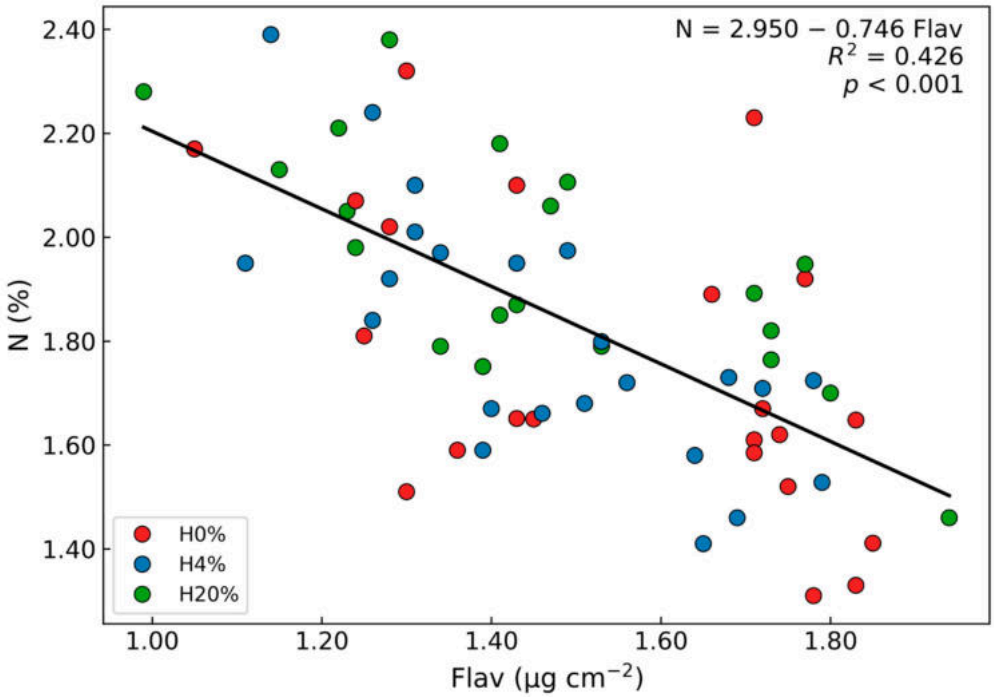

Figure 5. Relationship between flavonol content measured with the Dualex device (Flav) and leaf N content (N, %) obtained from chemical analyses in 'Nashi' pear leaves. Each point represents an individual plant, with colors indicating different Hoagland treatments (H0%, H4%, and H20%).

Since Flav accumulation reflects an integrated response to multiple physiological and environmental factors (and not exclusively to N nutritional status), the Flav content measured with the Dualex represents a composite signal. Nonetheless, in the present study, it displayed a better predictive ability compared with Chl content or Anth content, suggesting greater sensitivity in capturing variations in N% under field-like conditions. Similar results have been observed in grapevine [33]. The mixed-effects analysis confirmed the robustness of this relationship, as Flav remained significantly and negatively associated with N% after accounting for sampling date and repeated measurements on the same plants (Table 3). This result supports the use of Flav as an inverse optical indicator of N status, although its interpretation should consider that Flav accumulation can also respond to developmental and environmental factors.

A direct linear regression showed a direct relationship between NBI and N% (Figure 6), with N% increasing as NBI values increased. The coefficient of determination (R^2 = 0.480) indicated that NBI accounted for a larger proportion of the variability in N % than the other individual Dualex parameters, although a relevant portion of variability remained unexplained (Figure 6). This direct relationship between NBI and N % has been widely documented in the literature, particularly in cultivated herbaceous species such as wheat and maize, supporting the use of NBI as an integrated optical indicator of N nutritional status [76]. Validation studies of the Dualex device have shown that NBI correlates more closely with N% than Chl content or Flav content considered separately, owing to its ability to integrate information associated with multiple metabolic components of the leaf [78].

Field applications have also demonstrated that, although NBI is among the most robust optical indices for diagnosing N nutritional status, a significant portion of the variability in N% may remain unexplained, particularly in fruit tree species, where leaves of different age, position within the canopy, and light exposure generate pronounced physiological gradients within the plant [33]. Biologically, the observed relationship is consistent with the functional meaning of NBI, which reflects the balance between primary metabolism

processes associated with Chl synthesis and secondary metabolism linked to the accumulation of phenolic compounds, making a direct relationship with N% physiologically reasonable [77].

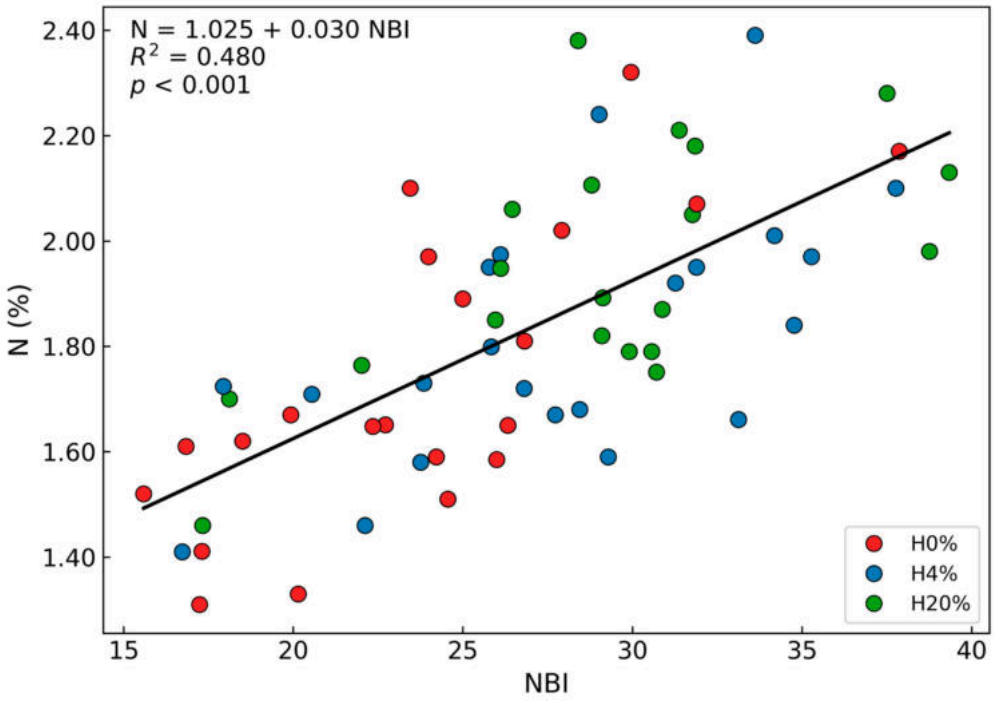

Figure 6. Relationship between the N Balance Index (NBI) and leaf N content (N, %) obtained from chemical analyses in 'Nashi' pear leaves. Each point represents an individual plant, with colors indicating different Hoagland treatments (H0%, H4%, and H20%).

This result was further supported by the mixed-effects model, in which NBI remained the most reliable proximal optical predictor of N% after accounting for sampling date and repeated measurements on the same plants (Table 3). Among the tested proximal optical parameters, the model including NBI showed the lowest prediction errors, confirming that NBI provided the most consistent information on leaf N status under the present experimental conditions.

However, although NBI showed the strongest association with leaf N content among the optical parameters, it remains limited, as the simple linear regression explained less than half of the observed variability. Therefore, NBI and the other optical parameters evaluated in this study should be considered useful mainly for detecting broad trends or relative differences in leaf N status, rather than for replacing laboratory chemical analyses totally.

3.1.2. CL-01 Chlorophyll Meter

Regarding the Chl content measured with the CL-01 device, no significant relationship with leaf N% was observed when data from the entire experimental period were included in the exploratory regression analysis (Figure 7A). This result was consistent with the mixed-effects model performed across all sampling dates, in which CL-01 was not significantly associated with leaf N% after accounting for sampling date and repeated measurements on the same plants (Table 3).

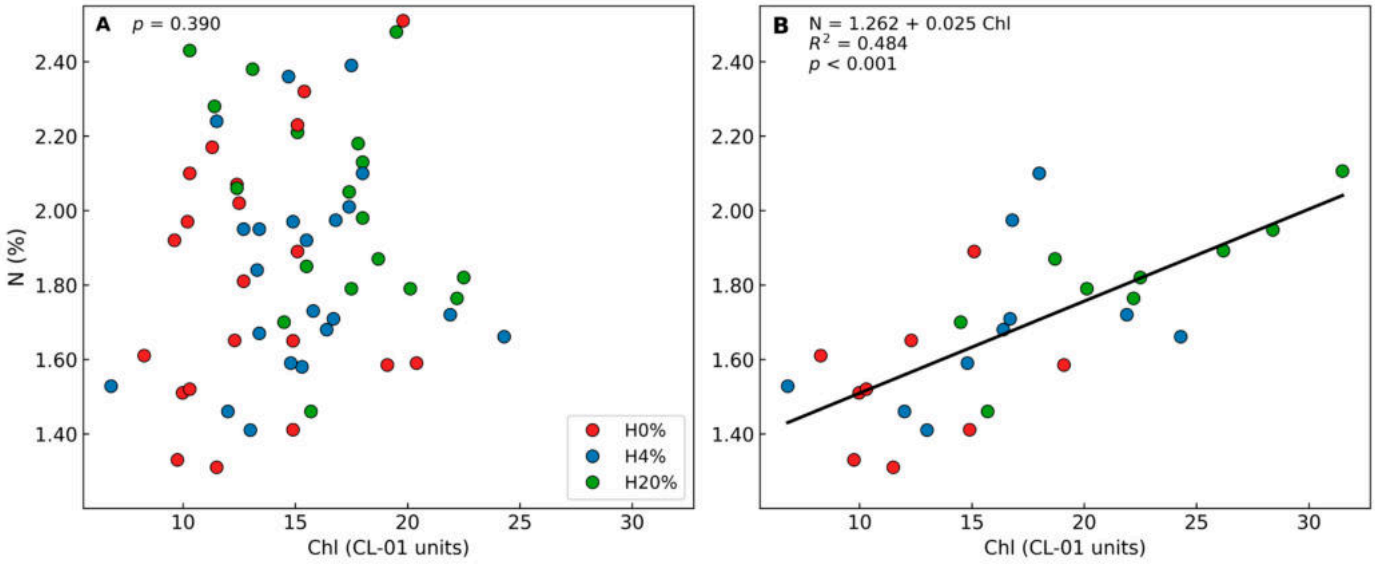

Figure 7. Relationship between leaf Chl content measured with the CL-01 Chlorophyll Meter (Chl) and leaf N content (N, %) determined through chemical analysis in 'Nashi' pear, using data from all sampling dates (**A**) or using only the data collected between 31 July and 29 August (**B**). Each point represents an individual plant, with colors indicating different Hoagland treatments (H0%, H4%, and H20%).

However, when the analysis was restricted to the later sampling dates, 31 July and 29 August, a direct linear relationship emerged between CL-01 Chl content and leaf N% (Figure 7B). In this restricted dataset, the coefficient of determination (R^2 = 0.484) indicated that CL-01 Chl content accounted for 48.4% of the variability in leaf N, although a relevant portion of variability remained unexplained. This pattern was confirmed by the restricted mixed-effects analysis performed on the same two sampling dates, in which CL-01 was significantly and positively associated with N% (β = 0.023, $p < 0.001$), with lower prediction errors than the model fitted across all dates (RMSE = 0.096; MAE = 0.076).

The direct relationship observed between N% and CL-01 Chl content measured on 31 July and 29 August is consistent with the results obtained using the Dualex device. This supports the interpretation that the N–Chl relationship becomes more evident when analyses are conducted on mature, physiologically stable leaves within phenologically uniform time windows. Conversely, CL-01 was not significantly associated with P or K in the same restricted analysis, suggesting that its potential usefulness was mainly related to N status under standardized sampling conditions [34,79].

3.1.3. Pocket PEA Fluorimeter

No significant relationship between the maximum photochemical efficiency of PSII (Fv/Fm) measured with the Pocket PEA and N% was found in the exploratory regression analysis (p = 0.249). This result was confirmed by the mixed-effects model, in which Fv/Fm was not significantly associated with N% after accounting for sampling date and repeated measurements on the same plants (Table 3). The Fv/Fm ratio is an indicator of the maximum functionality of PSII, with optimal values typically ranging from 0.75 to 0.85, and reflects how efficiently PSII uses absorbed light to drive photosynthesis by transferring electrons through the photosynthetic electron transport chain [80].

The absence of a correlation between Fv/Fm and leaf N% is expected, as maximum PSII efficiency is primarily an indicator of photosystem functionality in response to photo-oxidative stress rather than overall plant nutritional status [81]. Under non-limiting N conditions, Fv/Fm generally remains close to optimal values and declines only under severe

stress that damages or impairs PSII. The relatively moderate changes in N% observed in this study (approximately 1.3 to 2.5%) were therefore insufficient to appreciably affect PSII efficiency. Indeed, Fv/Fm remained mostly within the optimal range for young plants, indicating that they were not experiencing any severe stress [81,82]. Future experiments inducing more drastic changes in N% may be needed to see significant associations between Fv/Fm and N%.

3.1.4. Multispectral Vegetation Indices for Nitrogen

Since UAV-derived multispectral indices were available for only one sampling date, the relationships between vegetation indices and N% were analyzed using cross-sectional regressions. In the case of NDVI, the relationship with N% was linear and direct, with N% increasing as NDVI increased (Figure 8A). The regression was statistically significant, with $R^2 = 0.477$. Considering the relatively limited number of observations and the single-date nature of the multispectral acquisition, this result should be interpreted as an exploratory indication that NDVI captured part of the variability in plant N status. Furthermore, a substantial portion of the variability remained unexplained, suggesting that NDVI alone could not fully represent the complexity of nitrogen dynamics in the plant.

The NDVI is derived from the normalized difference between reflectance in the NIR and Red spectral regions. Also, reflectance in the Red region is strongly influenced by Chl content, as the latter absorbs a large fraction of the incoming radiation in this wavelength range. Moreover, Chl content typically increases with higher N availability, since N is a fundamental component of photosynthetic pigments and of proteins associated with the photosystems [83,84]. Consequently, higher N% levels tend to correspond to higher NDVI values due to enhanced Red-light absorption and increased canopy capacity to intercept incoming radiation [85]. However, in young potted plants, the rapid expansion of leaf area and shoot biomass may generate a marked dilution effect, reducing the concentration of N in the tissues even when nutrient supply is adequate [86,87]. Thus, NDVI should not be considered a direct estimator of nitrogen content, but rather a proxy of canopy vigor and Chl-related optical properties, which are only indirectly linked to plant N status. Several studies in the literature have investigated the estimation of N content using NDVI. In a study conducted on a 'RedBlush' pear orchard, several vegetation indices were calculated and compared with N% determined in the laboratory. At the leaf level, the most effective indices were NDVI and NDRE (720 nm), with R^2 values around 0.65 [31]. Similarly, in 'Huang-hua' pear leaves, NDVI (together with GNDVI and RVI) showed strong relationships with N%, with R^2 values ranging from 0.72 to 0.76 [88]. In our case, the relatively low R^2 of this study may be attributed to the fact that our experiment involved young potted plants with leaves still undergoing development, in which Chl content, and consequently N%, had not yet reached a stable level due to the lack of physiological maturity. Overall, considering both the evidence reported in the literature and our results, NDVI used alone provides only moderate reliability for association with N% in pear and is strongly dependent on the experimental context. Therefore, its use is more appropriate as a first-level indicator to be integrated with indices based on the Red Edge or SWIR regions and with calibrated spectral models to improve the explanatory capacity of leaf N estimates [38,89,90].

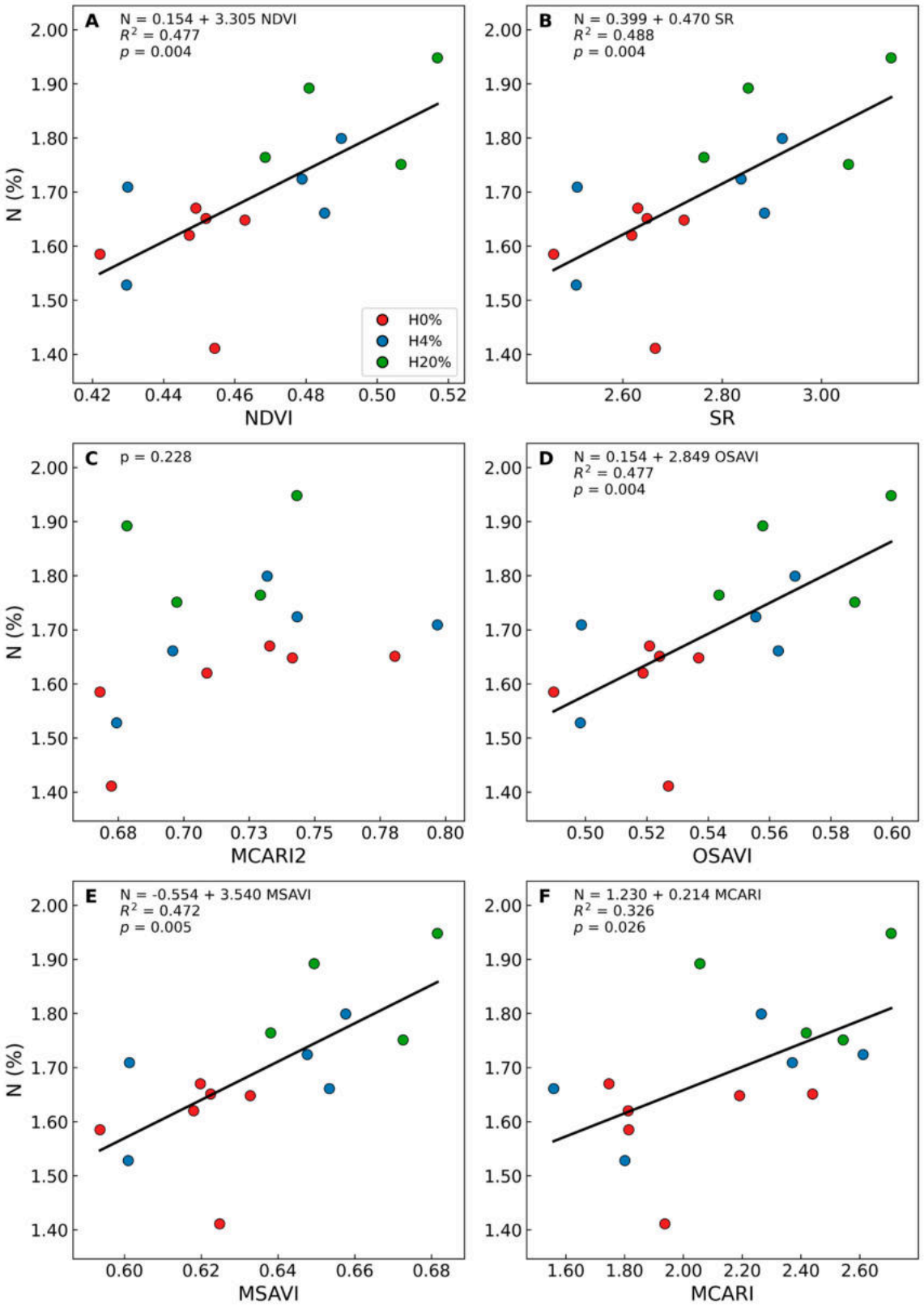

Figure 8. Relationships between leaf N content (N, %) and vegetation indices in 'Nashi' pear plants. Linear regressions are reported for Normalized Difference Vegetation Index (NDVI) (**A**), Simple Ratio (SR) (**B**), Modified Chlorophyll Absorption Ratio Index 2 (MCARI2) (**C**), Optimized Soil Adjusted Vegetation Index (OSAVI) (**D**), Modified Soil Adjusted Vegetation Index (MSAVI) (**E**), and Modified Chlorophyll Absorption in Reflectance Index (MCARI) (**F**). Each point represents an individual plant, with colors indicating different Hoagland treatments (H0%, H4%, and H20%).

Similarly to NDVI, SR showed a significant direct linear relationship with N% (Figure 8B). The slightly higher coefficient of determination (R^2 = 0.488) compared to NDVI suggests that SR may have captured canopy density and Chl-related variability slightly better under the present experimental conditions. This is consistent with the formulation of SR, which is based on the ratio between NIR and Red reflectance and is therefore directly linked to the amount of photosynthetically active vegetation. This behavior can be attributed to the strong absorption of Red radiation by Chl and the enhanced NIR reflectance resulting from leaf internal structure and canopy architecture [91]. Indeed, several studies have reported that simple ratio-based indices can enhance sensitivity to vegetation density compared to normalized indices. For example, Perry et al. [31] observed strong relationships between ratio-based vegetation indices (including NDVI and related formulations) and N% in pear orchards, highlighting their effectiveness in capturing canopy-level variability in N status. However, SR is known to be prone to saturation under conditions of high Chl content or dense canopies, which may limit its applicability in systems more developed than our young potted plants. This saturation effect can occur because, at high leaf area index or Chl levels, Red reflectance becomes minimal and NIR reflectance stabilizes, reducing the sensitivity of the index to further increases in biomass or Chl content [92]. In contrast, MCARI2 showed a weak and non-significant relationship with leaf N% (R^2 = 0.110, p = 0.228; Figure 8C). Although MCARI2 is designed to enhance sensitivity to Chl content while reducing the influence of canopy structure and soil background, this advantage was not evident under the present experimental conditions. This may be related to the limited number of observations, the single-date UAV acquisition, and the relatively low structural variability of young potted plants, in which leaf area and canopy architecture were not yet fully developed. Therefore, MCARI2 did not provide additional useful information for leaf N assessment in this study.

Similar to NDVI, OSAVI showed a significant positive relationship with N% (Figure 8D). This is consistent with the formulation of OSAVI, which introduces a soil adjustment factor to reduce background influence. However, in the present experimental setup, where plants were grown in pots and the spectral signal was primarily dominated by leaf reflectance, the contribution of soil background was likely limited. As a consequence, OSAVI did not provide a substantial improvement over NDVI, confirming that soil correction indices are more advantageous under field conditions with partial canopy cover, as widely reported in remote sensing studies [93]. Previous field studies have demonstrated that OSAVI can provide strong correlations with Chl-related parameters. For instance, in pear trees, UAV-based multispectral analyses showed that OSAVI, together with NDVI and SAVI, exhibited high correlations with leaf SPAD values (r coefficient ranging from 0.608 to 0.694), suggesting its sensitivity to canopy Chl content and vegetation vigor [94].

Another significant positive relationship with N% was shown by MSAVI (Figure 8E), with performance comparable to NDVI and OSAVI. Similar to OSAVI, MSAVI is designed to minimize soil effects, but its adaptive formulation may better account for variations in vegetation density. In this study, its performance remained moderate and comparable to NDVI. Nevertheless, considering the relatively limited number of observations and the controlled experimental conditions, this result can be regarded as consistent with a moderate exploratory association between spectral response and N%. At the same time, it suggests that factors other than background, such as leaf age, physiological variability, and N redistribution, may have played an important role in determining N%. Indeed, N is a highly mobile element within the plant, and its redistribution among tissues during growth can weaken the direct relationship between instantaneous spectral signals and leaf N content. This result partially agrees with previous findings reported in the literature. For instance, Roma et al. [95] observed that MSAVI was able to capture more nitrogen-

related information than NDVI and NDRE in olive canopies, highlighting its potential for improving N estimation under field conditions.

Finally, MCARI showed a significant but weaker relationship with N% compared to NDVI, SR, and OSAVI (Figure 8F). Although MCARI is specifically designed to estimate Chl content, its performance may be influenced by canopy structure and leaf optical properties. Variations in leaf thickness, water content, and developmental stage can alter reflectance independently of N content, introducing additional variability in the spectral signal [96]. In 'Red- blush' pear, Perry et al. [31] reported that MCARI showed lower predictive performance for N% compared to simpler indices such as NDVI, which achieved higher coefficients of determination (R^2 = 0.65 vs. 0.52 for MCARI). This suggests that, despite its specific design to isolate Chl absorption features, MCARI does not necessarily provide improved estimation of N%, particularly when structural and physiological variability dominate the spectral response.

Overall, the UAV-derived results should be interpreted with caution. Although NDVI, SR, OSAVI, and MSAVI showed significant relationships with N%, these analyses were based on a single UAV acquisition and approximately 18 plant-level observations. Therefore, they do not provide sufficient evidence for a stable or transferable nutrient diagnostic model. Rather, they indicate that, under the specific conditions and sampling date considered, some multispectral indices were able to capture part of the Chl variability associated with leaf N content. Additional UAV acquisitions across the growing season, larger plant populations, and independent validation datasets are required before UAV-derived vegetation indices can be considered reliable tools for nutrient diagnosis in pear trees.

3.1.5. Multiple Linear Regression Approach

The multiple linear regression analysis identified CL-01 Chl and Flav as selected predictors of N% ($p < 0.001$). The coefficient of determination (R^2 = 0.549) indicated that the model explained 54.9% of the variability in N%, while 45.1% remained unexplained. The root mean square error (RMSE = 0.180) indicated a moderate dispersion of data around the regression plane. This model was based on proximal measurements collected across four sampling dates and therefore included a broader temporal dataset than the single-date UAV-based analyses. However, because the model was fitted using an OLS framework and was not cross-validated, it should be interpreted only as an exploratory indication that Chl and Flav-related variables may provide complementary information on leaf N variability. Overall, the regression plane showed an increase in N% as CL-01 Chl content increased and Flav content decreased, suggesting a complementary contribution of these two optical variables in explaining N% variability (Figure 9). The positive contribution of Chl is consistent with the central physiological role of N in the biosynthesis of Chl and photosynthetic proteins, which represent a major fraction of leaf N, making this pigment a useful indicator of N nutritional status [97,98]. However, Chl signals can tend to saturate at very high N levels; therefore, Chl measurements alone may lose sensitivity for estimating N at its highest levels [99–101].

In contrast, Flav showed a negative association with N%, confirming their role as stress indicators under limited nutrient availability [101,102]. The combined behavior of Chl and Flav observed in this study reflects their opposite relationship with plant N status, as previously reported by Kaniszewski et al. [103], where Chl increased and Flav decreased with increasing N availability. This complementary response explains why high Chl associated with low Flav corresponds to higher N%, while the opposite pattern indicates N limitation. In wheat (*Triticum aestivum* L.) [76] and rice (*Oryza sativa* L.) [27], Chl and Flav exhibited different physiological response times to N status, contributing to an overall weak linear relationship.

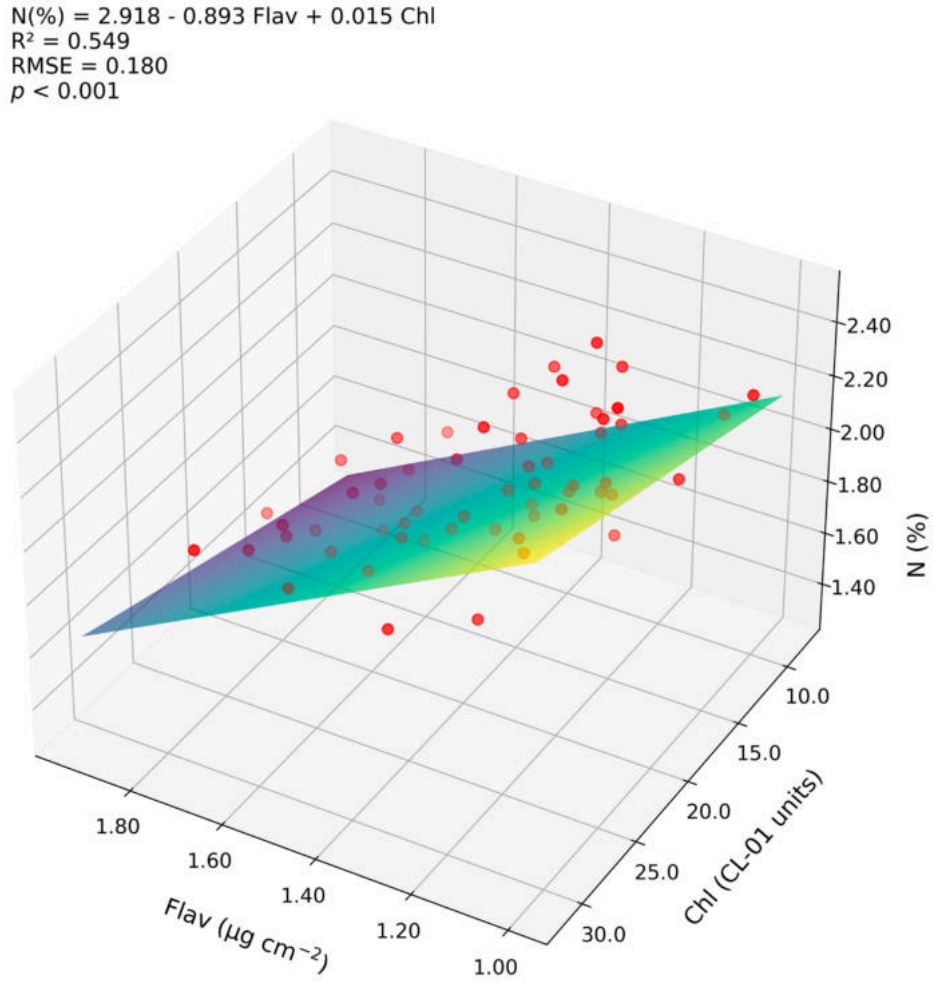

Figure 9. Three-dimensional relationship between leaf Chl content measured with the CL-01 device (Chl), flavonol content measured with the Dualex (Flav), and leaf N content (N, %) obtained from chemical analyses in 'Nashi' pear leaves. The surface represents the regression plane obtained from the multiple linear regression model, while the red points indicate the experimental observations.

However, this multiple regression model should be interpreted cautiously because it was based on an OLS framework and did not explicitly account for repeated measurements on the same plants. Therefore, the mixed-effects models were considered more appropriate for evaluating the robustness of individual proximal optical predictors. Accordingly, the multiple regression model should be regarded as an exploratory indication that the combination of Chl- and Flav-related information may improve N% estimation, rather than as a validated predictive model.

When applying a multiple linear regression approach using only vegetation indices, no significant relationships with N% were observed.

3.2. Phosphorus (P)

Leaf P content in the three Hoagland treatments (H0%, H4%, and H20%) showed a similar decreasing trend throughout the growing season (Figure 10). The highest values were observed at the first sampling date (8 May), with contents ranging between approximately 0.92 and 0.99 mg P g^{-1}, followed by a gradual decline at subsequent sampling dates, reaching the lowest values at the final sampling date (29 August), between approximately 0.59 and 0.63 mg P g^{-1}. No significant difference was detected among the three nutritional treatments overall or at any of the sampling dates.

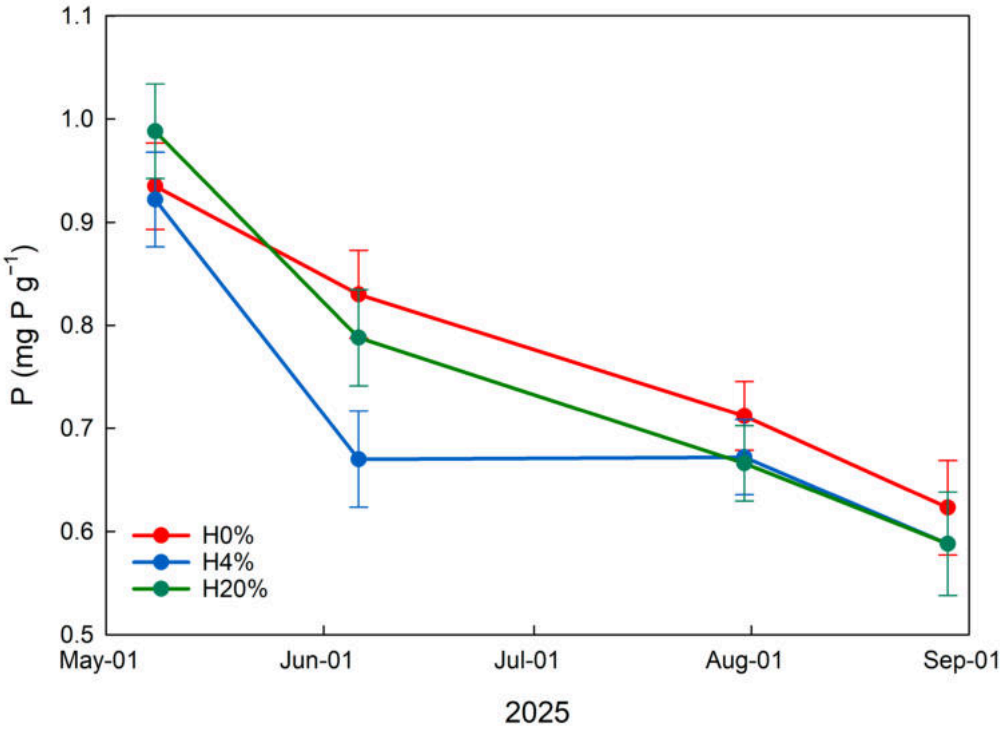

Figure 10. Leaf P content determined by chemical analysis in 'Nashi' pear leaves under the three Hoagland solution treatments (H0%, H4%, and H20%) during the trial period. Error bars represent the standard errors of the means. No significant differences were detected among treatments.

The P content at the beginning of the experiment was below the optimal range for pear leaves (1.2–2.0 mg P g^{-1}) [104], and despite the addition of the Hoagland nutrient solution, we could not bring P levels to the optimal range even in the H20% treatment. Nevertheless, the temporal variation in P observed during the experiment allowed us to perform data analyses and investigate correlations with the different parameters measured using optical devices.

The reduction in leaf P content observed over the season can be mainly attributed to a dilution effect associated with the rapid vegetative growth of young leaves [105,106]. During periods of intense leaf expansion and shoot development, biomass accumulation may occur more rapidly than the net accumulation of nutrients in plant tissues, resulting in a decrease in the concentration of mineral elements in the leaves [107,108]. The absence of significant differences among treatments suggests that, under our experimental conditions, P availability in the substrate did not represent a limiting factor for plant uptake. Overall, the results indicate that the variability in leaf P content was mainly driven by the seasonal growth dynamics of the plants rather than by differences in the applied fertilization levels.

Because leaf P content was mainly affected by temporal dynamics rather than by clear differences among fertilization treatments, the relationships between proximal optical parameters and leaf P were further evaluated using linear mixed-effects models (Table 4).

The mixed-effects models showed that none of the proximal optical parameters retained a significant association with leaf P (Table 4). Therefore, regression analyses should be interpreted as indicative and exploratory, rather than as evidence of a robust diagnostic capability for P status.

Table 4. Linear mixed-effects model results for the relationships between proximal optical parameters (Chl: Chl measured with Dualex; Flav: flavonols measured with Dualex; Anth: anthocyanin measured with Dualex; NBI: Nitrogen Balance Index measured with Dualex; Fv/Fm: maximum quantum efficiency of photosystem II measured with Pocket PEA; CL-01: Chl measured with CL-01 Chlorophyll Meter; CL-01 Filtered: Chl measured with CL-01 Chlorophyll Meter in the last two sampling dates) and Leaf P content. For each optical predictor, β indicates the slope of each optical predictor, SE the standard error, RMSE the root mean square error, and MAE the mean absolute error.

Predictor	β	SE	*p*-Value	RMSE	MAE
Chl	0.000	0.003	0.940	0.080	0.062
Flav	−0.086	0.077	0.268	0.079	0.059
Anth	−0.043	0.219	0.845	0.079	0.062
NBI	0.003	0.003	0.257	0.081	0.061
Fv/Fm	0.288	0.260	0.268	0.079	0.061
CL-01	−0.002	0.003	0.537	0.081	0.065

3.2.1. Dualex and CL-01 Chlorophyll Meter

No significant relationships were observed between leaf P content and Anth or Chl content measured with the Dualex device or Chl content measured with the CL-01 Chlorophyll Meter. These results were confirmed by the mixed-effects models, in which none of these parameters retained a significant association with leaf P after accounting for sampling date and repeated measurements on the same plants. Unlike N, which is a structural component of Chl molecules and photosynthetic proteins, P mainly participates in energy transfer processes (ATP synthesis) [109], phosphorylation reactions, and carbon metabolism, rather than directly influencing pigment biosynthesis [110]. Consequently, variations in leaf P content are not necessarily reflected in changes in Chl levels [111]. Similarly, Anth accumulation is generally associated with severe physiological stress or strong imbalances in carbon–N metabolism, conditions that were not evident within the range of P variation observed in this study [112,113]. As a result, the optical signals related to Chl and Anth measured with the Dualex were not sensitive to the differences in leaf P content recorded during the experiment.

Initial regression analyses indicated indicative relationships between leaf P content and some Dualex-derived parameters, particularly Flav and NBI. However, these relationships were not confirmed in the linear mixed-effects models. Therefore, they were not considered robust and are not interpreted as reliable indicators of leaf P status.

Under P deficiency, changes in energy metabolism, photosynthetic activity, and carbon allocation may favor the synthesis of secondary metabolites, including Flav [114,115]. However, in the present study, the absence of clear treatment-induced differences in leaf P content and the lack of confirmation in the mixed-effects framework suggest that Flav responses were likely influenced by temporal dynamics, interactions with other nutrients, or broader physiological adjustments rather than by P status alone. In this context, the increase in Flav content detected by the Dualex device may reflect a physiological adjustment of leaf metabolism to variations in nutrient availability.

The weak association initially observed between leaf P content and NBI may be partly related to the formulation of NBI, which is calculated as the ratio between Chl and Flav. However, since this relationship was not confirmed by the mixed-effects model, it should not be interpreted as a robust indicator of leaf P status.

3.2.2. Pocket PEA

The relationship between leaf P content and the maximum photochemical efficiency of PSII (Fv/Fm) measured with Pocket PEA did not show a statistically significant correlation ($p = 0.130$). This result was confirmed by the linear mixed-effects model, in which Fv/Fm

was not significantly associated with leaf P content after accounting for sampling date and repeated measurements on the same plants. This suggests that variations in leaf P content were not associated with detectable changes in the maximum efficiency of PSII during the experimental period.

This result is physiologically reasonable, as the Fv/Fm ratio represents the maximum quantum efficiency of PSII and is primarily used as an indicator of photoinhibition or severe physiological stress affecting the photosynthetic apparatus [80,81]. Under non-stressful conditions, Fv/Fm values typically remain relatively stable within a narrow range (approximately 0.75–0.85), reflecting a normally functioning photosynthetic system [116,117]. In the present experiment, most of the measured values fall within this optimal range, indicating that the plants were not experiencing significant photo-inhibitory stress that could affect PSII performance.

Phosphorus plays an essential role in plant metabolism, particularly in energy transfer processes such as ATP synthesis and phosphorylation reactions involved in photosynthesis [9]. However, moderate variations in leaf P content do not necessarily translate into immediate changes in the photochemical efficiency of PSII [118,119]. Therefore, under the present experimental conditions, Fv/Fm did not provide a reliable optical indicator of leaf P status.

3.2.3. Multispectral Vegetation Indices for Phosphorus

In contrast to N, leaf P content showed weaker relationships with multispectral variables. Since UAV-derived multispectral data were available for only one sampling date, these relationships were assessed using cross-sectional regression analyses and should be interpreted with caution. Among the tested predictors, only reflectance in the Red and Green bands exhibited statistically significant relationships with leaf P content, although the coefficients of determination were relatively low (Figure 11A,B). The direct relationships observed with Red and Green reflectance may be indirectly related to changes in leaf optical properties associated with P deficiency. Phosphorus plays a key role in energy transfer, ATP synthesis, and overall metabolic activity, and its deficiency can lead to reduced photosynthetic efficiency and altered pigment composition [120,121]. In particular, P deficiency has been associated with reductions in Chl content, which may increase reflectance in the visible region, especially in the Green and Red wavelengths [122]. However, these effects are typically indirect and less pronounced than those associated with N, resulting in weaker spectral relationships [123]. Consistently with this interpretation, none of the vegetation indices calculated in the previous analysis showed significant relationships with leaf P content. This result is in line with previous studies, which have highlighted that most vegetation indices are primarily sensitive to Chl content and therefore more closely related to N rather than P status [124,125]. Zhao et al. [92] reported that indices such as MCARI and TCARI are primarily driven by Chl-related variations and may show only weak relationships with biochemical parameters not directly involved in pigment composition. This further supports the limited capability of broadband multispectral indices to capture P variability. Indeed, vegetation indices are largely based on the contrast between visible absorption (mainly driven by Chl) and near-infrared reflectance, making them inherently more responsive to variations in pigments than to nutrients such as P that do not directly contribute to light absorption processes [126]. This supports the limited capability of broadband multispectral indices to capture P-related variability.

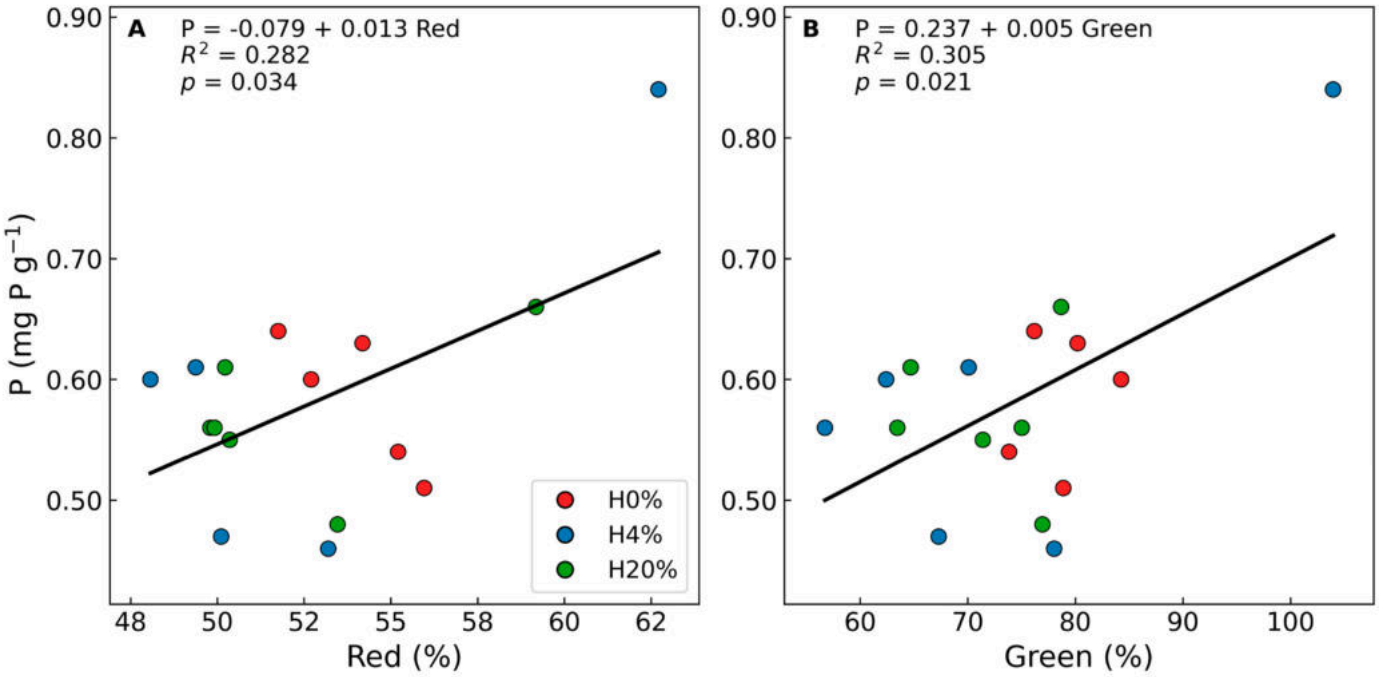

Figure 11. Relationships between reflectance in the Red (**A**) and Green (**B**) spectral bands and leaf P content obtained from chemical analyses of 'Nashi' pear leaves. Each point represents an individual plant, with colors indicating different Hoagland treatments (H0%, H4%, and H20%).

Furthermore, the use of young potted plants may have contributed to the limited performance of spectral indicators. In such conditions, rapid growth dynamics, nutrient redistribution, and potential dilution effects can introduce additional variability in tissue nutrient content that is not directly reflected in canopy spectral properties. More specifically, although the experimental setup reduced environmental variability compared to field conditions, the sparse and partially developed canopy of young potted plants may have increased the influence of background signals and limited canopy closure. This condition can reduce the sensitivity of spectral indices, which rely on canopy structure and density to enhance signal contrast [31]. Moreover, the relatively homogeneous canopy structure and limited variability of plant biomass reduce the sensitivity of spectral indices that rely on structural differences [96].

Overall, these results indicate that the estimation of P status using multispectral data alone was limited under the present experimental conditions. While simple reflectance in the visible bands may provide preliminary indications of P-related physiological changes, the observed relationships were weak and based on a single acquisition date. More accurate assessment of P status would likely require independent P gradients, repeated spectral acquisitions, and the integration of additional information, such as hyperspectral data, fluorescence measurements, or direct plant-based sensing approaches.

3.3. Potassium (K)

The leaf K content showed relatively high variation and, overall, a similar trend for all treatments during the growing season (Figure 12). The highest values were observed at the first sampling date (8 May), with contents ranging between 8.4 and 9.7 mg g^{-1}. Leaf K content reached the lowest value on 31 July, particularly in the H4% treatment where values dropped to about 5.8 mg g^{-1}. A slight, non-significant increase in K content was observed in the last sampling date (29 August). In pear trees, adequate leaf K contents generally range between 10 and 15 mg g^{-1} of dry weight [127]. Although values in our

trial (5.8 to 9.7 mg g^{-1}) were somewhat below the optimal range generally reported for pear leaves, they were not low enough to induce clear deficiency symptoms.

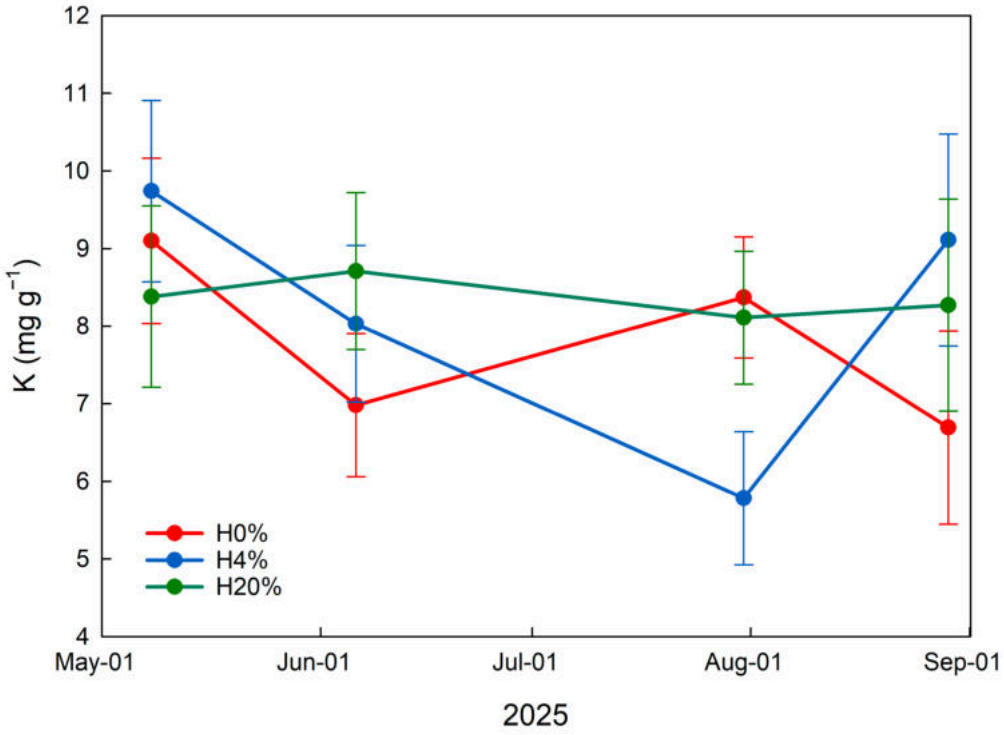

Figure 12. Leaf K content determined by chemical analysis in 'Nashi' pear leaves under the three Hoagland solution treatments (H0%, H4%, and H20%) during the trial period. Error bars represent the standard errors of the means. No significant differences were detected among treatments.

The statistical analysis revealed significant differences among sampling dates, indicating a seasonal variation in leaf K content. In contrast, no significant differences were detected among the three nutritional treatments or the interaction with dates. This suggests that the fertilization treatments applied with the Hoagland solutions did not produce a clear distinction in leaf K content under the experimental conditions considered.

Proximal optical parameters and leaf K content were evaluated using linear mixed-effects models (Table 5). The linear mixed-effects models showed that most proximal optical parameters were not significantly associated with leaf K content. Chl, Flav, Anth, NBI, and CL-01 did not retain significant relationships with K. Only Fv/Fm showed a statistically significant association; however, this isolated result should be interpreted with caution because of the limited model performance and the lack of a direct physiological link between K concentration and maximum PSII photochemical efficiency. Therefore, no robust proximal optical predictor of leaf K content was identified under the present experimental conditions.

As for the other nutrients, the seasonal decrease in leaf K content observed during midsummer can be attributed to a dilution effect associated with the rapid vegetative growth of young plants [127]. During periods of intense shoot elongation and leaf expansion, biomass accumulation may occur faster than nutrient uptake, leading to a reduction in the concentration of mineral elements within the leaf tissues [128]. Potassium is a highly mobile element within the plant and plays a crucial role in several physiological processes, including osmotic regulation, stomatal control, and carbohydrate transport [129,130]. As vegetative growth progresses, K may be redistributed among different plant organs, contributing to fluctuations in leaf content over time [131].

Table 5. Linear mixed-effects model results for the relationships between proximal optical parameters (Chl: Chl measured with Dualex; Flav: flavonols measured with Dualex; Anth: anthocyanin measured with Dualex; NBI: Nitrogen Balance Index measured with Dualex; Fv/Fm: maximum quantum efficiency of photosystem II measured with Pocket PEA; CL-01: Chl measured with CL-01 Chlorophyll Meter; CL-01 Filtered: Chl measured with CL-01 Chlorophyll Meter in the last two sampling dates) and Leaf K content. For each optical predictor, β indicates the slope of each optical predictor, SE the standard error, RMSE the root mean square error, and MAE the mean absolute error.

Predictor	β	SE	*p*-Value	RMSE	MAE
Chl	0.016	0.053	0.770	2.244	1.906
Flav	−2.113	1.820	0.246	2.368	1.973
Anth	1.653	5.747	0.778	2.405	2.022
NBI	0.068	0.057	0.262	2.168	1.824
Fv/Fm	−13.616	6.428	0.034	2.246	1.910
CL-01	−0.069	0.074	0.352	2.380	2.001

Overall, the proximal optical parameters showed limited sensitivity to leaf K content. This result is consistent with the physiological role of K in plant metabolism. Unlike N, K is not incorporated into structural organic compounds such as Chl, amino acids, or proteins but mainly acts as a soluble cation involved in osmotic regulation, stomatal functioning, enzyme activation, and ionic balance [44,132]. Consequently, moderate variations in leaf K content are not expected to directly affect pigment biosynthesis or phenolic compound accumulation, which represent the main optical signals detected by Dualex and CL-01. Similarly, Fv/Fm primarily reflects the maximum photochemical efficiency of PSII and generally changes under severe stress affecting the photosynthetic apparatus [44,133]. Moderate variations in K content, such as those observed in the present study, are unlikely to induce measurable changes in PSII efficiency in plants growing under non-stressful conditions. Therefore, the observed association may reflect indirect physiological variation rather than a specific optical response to K status.

No significant relationships were observed between leaf K content and any vegetation index. This result suggests that K status could not be reliably estimated using multispectral reflectance data. This finding is consistent with the physiological role of K in plants. As mentioned above, K does not contribute to pigment composition [134]. Therefore, variations in K content do not directly induce detectable changes in leaf optical properties, particularly in the visible and near-infrared regions commonly used for vegetation indices [135]. Indeed, spectral approaches have shown lower sensitivity to nutrients that are not directly linked to pigment-related optical signals [11]. For instance, VIS–NIR spectroscopy and multispectral imaging have been demonstrated to be highly effective for estimating N and Chl-related traits, while their performance decreases for other nutrients due to weaker spectral signatures [136].

This limitation has also been highlighted in recent studies focusing on K detection. For example, Yu et al. [137] reported that K exhibits a distinct spectral behavior mainly associated with indirect effects such as water status and molecular vibrations, rather than strong direct absorption features in the visible spectrum, making its detection more challenging compared to N. Similarly, their results showed that accurate estimation of leaf K required advanced approaches such as NIR spectroscopy combined with machine learning, rather than simple reflectance-based indices.

Overall, these results confirm that K status is inherently difficult to assess through reflectance-based approaches alone. This limitation has been widely reported in the literature, where K is generally considered one of the least detectable macronutrients using remote sensing techniques, particularly when relying on broadband multispectral indices.

3.4. Limitations

This study has some limitations that should be considered when interpreting the results. The experiment was conducted on a relatively small number of young potted 'Nashi' pear trees, and UAV-derived multispectral data were collected on a single date. These aspects limit the robustness and generalizability of the observed relationships and indicate that UAV-based results should be interpreted as exploratory associations rather than as robust relationships. Moreover, the reported associations were not tested across different seasons, cultivars, orchard conditions, or environmental contexts. The analytical approach also mainly relied on vegetation indices and univariate relationships, which may not fully exploit the multidimensional information contained in proximal optical, Chl fluorescence, and UAV-derived multispectral data. Therefore, the optical responses observed in this study should be considered context-specific and preliminary. Future studies should include larger plant populations, repeated UAV acquisitions across the growing season, independent nutrient gradients, different cultivars and orchard systems, multivariate or chemometric approaches, and independent validation datasets to evaluate robustness, temporal stability, and transferability of optical indicators for nutrient assessment in orchard.

4. Conclusions

This study provides an explorative, comprehensive approach integrating proximal optical sensing, Chl fluorescence measurements, and UAV-derived multispectral information within the same experimental framework for the non-destructive assessment of nutrient variability in potted 'Nashi' pear plants. As expected, the associations with the highest coefficient of determination were observed for N%, particularly with pigment-related optical parameters such as Chl, Flav, and NBI, as well as selected multispectral vegetation indices. Linear mixed-effects models showed that NBI, Flav, and, to a lesser extent, Chl retained the strongest associations with N% among the tested proximal optical parameters. The CL-01 chlorophyll meter showed relevant associations only when measurements were restricted to the later sampling dates, suggesting the importance of leaf maturity and sampling standardization.

In contrast, the optical parameters evaluated in this study showed limited sensitivity to leaf P and K contents under the experimental conditions tested. The mixed-effects models did not confirm the few linear relationships observed for P or K, indicating that these nutrients were less directly captured by the optical approaches used. These weaker associations may be partly explained by the limited nutrient variability induced by the treatments and by the indirect physiological links between P or K and optical responses. Overall, integrated proximal and UAV-based optical sensing approaches may provide preliminary support for monitoring nutrient-related variability in 'Nashi' pear trees, particularly for leaf N-associated pigment responses, while further validation is required for P and K assessment. Future studies should include broader seasonal datasets, mature orchard conditions, independent nutrient gradients, and advanced sensing and modeling approaches to improve the robustness and transferability of nutrient assessment approaches in fruit tree systems.

Supplementary Materials: The following supporting information can be downloaded at: https://www.mdpi.com/article/10.3390/horticulturae12070785/s1, Figure S1: Daily mean air temperature (°C) (red line) and relative humidity (%) (blue line) recorded from 8 May to 29 August 2025; Figure S2: Daily mean solar radiation recorded from 8 May to 29 August 2025.

Author Contributions: Conceptualization, P.T.B.F. and R.L.B.; methodology, P.T.B.F., S.M.M., A.C. and R.L.B.; validation, P.T.B.F., A.C. and R.L.B.; formal analysis, P.T.B.F., A.C., S.M.M. and R.L.B.; investigation, P.T.B.F., A.C., R.M. and S.M.M.; resources, R.M. and R.L.B.; data curation, P.T.B.F., A.C., S.M.M. and R.M.; writing—original draft preparation, P.T.B.F.; writing—review and editing, P.T.B.F., A.C., R.M., S.M.M., A.M. and R.L.B.; visualization, P.T.B.F., A.C., R.M., S.M.M. and A.M.; supervision, R.M., S.M.M. and R.L.B.; funding acquisition, R.L.B. All authors have read and agreed to the published version of the manuscript.

Funding: This research was funded by the following projects: SUSTAINABLE project, funded by the European Union's Horizon 2020 research and innovation program under the Marie SklodowskaCurie-RISE Grant Agreement No. 101007702 (https://www.projectsustainable.eu, accessed on 5 January 2025); Ecosistema dell'innovazione Sicilian MicronanoTech Research and Innovation Center (SAMOTHRACE) and Fondo Finalizzato alla Ricerca di Ateneo FFR_D13_008811, funded by Ministero dell'Università e della Ricerca (MUR), Grant Agreement No. ECS_00000022.

Data Availability Statement: The original contributions presented in this study are included in the article/Supplementary Materials. Further inquiries can be directed to the corresponding authors.

Conflicts of Interest: The authors declare no conflicts of interest.

References

1. Falcon, W.P.; Naylor, R.L.; Shankar, N.D. Rethinking Global Food Demand for 2050. *Popul. Dev. Rev.* **2022**, *48*, 921–957. [CrossRef]
2. Gatto, A.; Chepeliev, M. Global Food Loss and Waste Estimates Show Increasing Nutritional and Environmental Pressures. *Nat. Food* **2024**, *5*, 136–147. [CrossRef]
3. Cheng, P.; Zhang, Y.; Liu, K.; Kong, X.; Wu, S.; Yan, H.; Jiang, P. Continuing the Continuous Harvests of Food Production: From the Perspective of the Interrelationships among Cultivated Land Quantity, Quality, and Grain Yield. *Humanit. Soc. Sci. Commun.* **2025**, *12*, 46. [CrossRef]
4. Penuelas, J.; Coello, F.; Sardans, J. A Better Use of Fertilizers Is Needed for Global Food Security and Environmental Sustainability. *Agric. Food Secur.* **2023**, *12*, 5. [CrossRef]
5. Liu, X.; Beusen, A.H.W.; van Grinsven, H.J.M.; Wang, J.; van Hoek, W.J.; Ran, X.; Mogollón, J.M.; Bouwman, A.F. Impact of Groundwater Nitrogen Legacy on Water Quality. *Nat. Sustain.* **2024**, *7*, 891–900. [CrossRef]
6. Hawkesford, M.J.; Cakmak, I.; Coskun, D.; De Kok, L.J.; Lambers, H.; Schjoerring, J.K.; White, P.J. Functions of macronutrients. In *Marschner's Mineral Nutrition of Plants*; Academic Press: Cambridge, MA, USA, 2023; pp. 201–281.
7. Sinha, D.; Tandon, P.K. An Overview of Nitrogen, Phosphorus and Potassium: Key Players of Nutrition Process in Plants. In *Sustainable Solutions for Elemental Deficiency and Excess in Crop Plants*; Mishra, K., Tandon, P.K., Srivastava, S., Eds.; Springer: Singapore, 2020; pp. 85–117, ISBN 978-981-15-8636-1.
8. Wang, Q.; Li, S.; Li, J.; Huang, D. The Utilization and Roles of Nitrogen in Plants. *Forests* **2024**, *15*, 1191. [CrossRef]
9. Rychter, A.M.; Rao, I.M. Role of phosphorus in photosynthetic carbon metabolism. In *Handbook of Photosynthesis*; Pessarakli, M., Ed.; Taylor and Francis Group, LLC: Tucson, AZ, USA, 2005; pp. 123–148, ISBN 978-131-537-213-6.
10. Jaiswal, D.K.; Verma, J.P.; Prakash, S.; Meena, V.S.; Meena, R.S. Potassium as an Important Plant Nutrient in Sustainable Agriculture: A State of the Art. In *Potassium Solubilizing Microorganisms for Sustainable Agriculture*; Meena, V.S., Maurya, B.R., Verma, J.P., Meena, R.S., Eds.; Springer: New Delhi, India, 2016; pp. 21–29, ISBN 978-81-322-2776-2.
11. Zahir, S.A.D.M.; Jamlos, M.F.; Omar, A.F.; Jamlos, M.A.; Mamat, R.; Muncan, J.; Tsenkova, R. Review—Plant Nutritional Status Analysis Employing the Visible and near-Infrared Spectroscopy Spectral Sensor. *Spectrochim. Acta Part A Mol. Biomol. Spectrosc.* **2024**, *304*, 123273. [CrossRef] [PubMed]
12. Oliveira, S.R.; Gomes Neto, J.A.; Nóbrega, J.A.; Jones, B.T. Determination of Macro- and Micronutrients in Plant Leaves by High-Resolution Continuum Source Flame Atomic Absorption Spectrometry Combining Instrumental and Sample Preparation Strategies. *Spectrochim. Acta Part B At. Spectrosc.* **2010**, *65*, 316–320. [CrossRef]
13. Manickam, S.; Rajagopalan, V.R.; Kambale, R.; Rajasekaran, R.; Kanagarajan, S.; Muthurajan, R. Plant Metabolomics: Current Initiatives and Future Prospects. *Curr. Issues Mol. Biol.* **2023**, *45*, 8894–8906. [CrossRef] [PubMed]
14. Lilay, G.H.; Persson, D.P.; Castro, P.H.; Liao, F.; Alexander, R.D.; Aarts, M.G.M.; Assunção, A.G.L. Arabidopsis bZIP19 and bZIP23 Act as Zinc Sensors to Control Plant Zinc Status. *Nat. Plants* **2021**, *7*, 137–143. [CrossRef] [PubMed]
15. Kalaji, H.M.; Bąba, W.; Gediga, K.; Goltsev, V.; Samborska, I.A.; Cetner, M.D.; Dimitrova, S.; Piszcz, U.; Bielecki, K.; Karmowska, K.; et al. Chlorophyll Fluorescence as a Tool for Nutrient Status Identification in Rapeseed Plants. *Photosynth. Res.* **2018**, *136*, 329–343. [CrossRef] [PubMed]

16. Bulacio Fischer, P.T.; Carella, A.; Massenti, R.; Fadhilah, R.; Bianco, R.L. Advances in Monitoring Crop and Soil Nutrient Status: Proximal and Remote Sensing Techniques. *Horticulturae* **2025**, *11*, 182. [CrossRef]
17. Kent Shannon, D.; Clay, D.E.; Sudduth, K.A. An Introduction to Precision Agriculture. In *Precision Agriculture Basics*; John Wiley & Sons, Ltd.: Hoboken, NJ, USA, 2018; pp. 1–12, ISBN 978-0-89118-367-9.
18. Chen, C.; Pan, J.; Lam, S.K. A Review of Precision Fertilization Research. *Environ. Earth Sci.* **2014**, *71*, 4073–4080. [CrossRef]
19. Fageria, N.K.; Moreira, A. Chapter Four—The Role of Mineral Nutrition on Root Growth of Crop Plants. In *Advances in Agronomy*; Sparks, D.L., Ed.; Academic Press: Cambridge, MA, USA, 2011; Volume 110, pp. 251–331.
20. Baret, F.; Guyot, G. Potentials and Limits of Vegetation Indices for LAI and APAR Assessment. *Remote Sens. Environ.* **1991**, *35*, 161–173. [CrossRef]
21. Jacquemoud, S.; Verhoef, W.; Baret, F.; Bacour, C.; Zarco-Tejada, P.J.; Asner, G.P.; François, C.; Ustin, S.L. PROSPECT + SAIL Models: A Review of Use for Vegetation Characterization. *Remote Sens. Environ.* **2009**, *113*, S56–S66. [CrossRef]
22. Moustaka, J.; Moustakas, M. Early-Stage Detection of Biotic and Abiotic Stress on Plants by Chlorophyll Fluorescence Imaging Analysis. *Biosensors* **2023**, *13*, 796. [CrossRef] [PubMed]
23. Mulla, D.J. Twenty Five Years of Remote Sensing in Precision Agriculture: Key Advances and Remaining Knowledge Gaps. *Biosyst. Eng.* **2013**, *114*, 358–371. [CrossRef]
24. Rouse, J.W.; Haas, R.H.; Schell, J.A.; Deering, D.W. Monitoring vegetation systems in the Great Plains with ERTS. In *Proceedings of the Third Earth Resources Technology Satellite (ERTS) Symposium, Washington, DC, USA, 10–14 December 1973*; NASA: Washington, DC, USA, 1973; Volume 1, pp. 309–317.
25. Li, D.; Zhang, P.; Chen, T.; Qin, W. Recent Development and Challenges in Spectroscopy and Machine Vision Technologies for Crop Nitrogen Diagnosis: A Review. *Remote Sens.* **2020**, *12*, 2578. [CrossRef]
26. Huete, A.; Didan, K.; Miura, T.; Rodriguez, E.P.; Gao, X.; Ferreira, L.G. Overview of the Radiometric and Biophysical Performance of the MODIS Vegetation Indices. *Remote Sens. Environ.* **2002**, *83*, 195–213. [CrossRef]
27. Zhang, K.; Liu, X.; Ma, Y.; Zhang, R.; Cao, Q.; Zhu, Y.; Cao, W.; Tian, Y. A Comparative Assessment of Measures of Leaf Nitrogen in Rice Using Two Leaf-Clip Meters. *Sensors* **2019**, *20*, 175. [CrossRef] [PubMed]
28. Gabriel, J.L.; Quemada, M.; Alonso-Ayuso, M.; Lizaso, J.I.; Martín-Lammerding, D. Predicting N Status in Maize with Clip Sensors: Choosing Sensor, Leaf Sampling Point, and Timing. *Sensors* **2019**, *19*, 3881. [CrossRef] [PubMed]
29. Giorio, P.; Nuzzo, V.; Guida, G.; Albrizio, R. Black Leaf-Clips of a Commercial Fluorometer Increased Leaf Temperature during Dark Adaptation under High Solar Radiation. *Photosynthetica* **2012**, *50*, 467–471. [CrossRef]
30. Vlaović, J.; Balen, J.; Grgić, K.; Žagar, D.; Galić, V.; Šimić, D. An Overview of Chlorophyll Fluorescence Measurement Process, Meters and Methods. In Proceedings of the 2020 International Conference on Smart Systems and Technologies (SST), Osijek, Croatia, 14–16 October 2020; pp. 245–250.
31. Perry, E.M.; Goodwin, I.; Cornwall, D. Remote Sensing Using Canopy and Leaf Reflectance for Estimating Nitrogen Status in Red-Blush Pears. *HortScience* **2018**, *53*, 78–83. [CrossRef]
32. Treder, W.; Klamkowski, K.; Kowalczyk, W.; Sas, D.; Wójcik, K. Possibilities of Using Image Analysis to Estimate the Nitrogen Nutrition Status of Apple Trees. *Zemdirbyste-Agriculture* **2016**, *103*, 319–326. [CrossRef]
33. Cerovic, Z.G.; Ghozlen, N.B.; Milhade, C.; Obert, M.; Debuisson, S.; Moigne, M.L. Nondestructive Diagnostic Test for Nitrogen Nutrition of Grapevine (*Vitis vinifera* L.) Based on Dualex Leaf-Clip Measurements in the Field. *J. Agric. Food Chem.* **2015**, *63*, 3669–3680. [CrossRef] [PubMed]
34. Padilla, F.M.; Gallardo, M.; Peña-Fleitas, M.T.; De Souza, R.; Thompson, R.B. Proximal Optical Sensors for Nitrogen Management of Vegetable Crops: A Review. *Sensors* **2018**, *18*, 2083. [CrossRef] [PubMed]
35. Muñoz-Huerta, R.F.; Guevara-Gonzalez, R.G.; Contreras-Medina, L.M.; Torres-Pacheco, I.; Prado-Olivarez, J.; Ocampo-Velazquez, R.V. A Review of Methods for Sensing the Nitrogen Status in Plants: Advantages, Disadvantages and Recent Advances. *Sensors* **2013**, *13*, 10823–10843. [CrossRef] [PubMed]
36. Neto, C.B.; Carranca, C.; Clemente, J.; de Varennes, A. Assessing the Nitrogen Nutritional Status of Young Non-Bearing 'Rocha' Pear Trees Grown in a Mediterranean Region by Using a Chlorophyll Meter. *J. Plant Nutr.* **2011**, *34*, 627–639. [CrossRef]
37. Xi, R.; Gu, Y.; Zhang, X.; Ren, Z. Nitrogen Monitoring and Inversion Algorithms of Fruit Trees Based on Spectral Remote Sensing: A Deep Review. *Front. Plant Sci.* **2024**, *15*, 1489151. [CrossRef] [PubMed]
38. Wang, J.; Shen, C.; Liu, N.; Jin, X.; Fan, X.; Dong, C.; Xu, Y. Non-Destructive Evaluation of the Leaf Nitrogen Concentration by In-Field Visible/Near-Infrared Spectroscopy in Pear Orchards. *Sensors* **2017**, *17*, 538. [CrossRef] [PubMed]
39. Zhu, G.; Wang, Q.; Zhang, S.; Guo, T.; Liu, S.; Lu, J. A Meta-Analysis of Crop Leaf Nitrogen, Phosphorus and Potassium Content Estimation Based on Hyperspectral and Multispectral Remote Sensing Techniques. *Field Crops Res.* **2025**, *329*, 109961. [CrossRef]
40. Yaryura, P.; Cordon, G.; Leon, M.; Kerber, N.; Pucheu, N.; Rubio, G.; García, A.; Lagorio, M. Effect of Phosphorus Deficiency on Reflectance and Chlorophyll Fluorescence of Cotyledons of Oilseed Rape (*Brassica napus* L.). *J. Agron. Crop. Sci.* **2009**, *195*, 186–196. [CrossRef]

41. Serbin, S.P.; Dillaway, D.N.; Kruger, E.L.; Townsend, P.A. Leaf Optical Properties Reflect Variation in Photosynthetic Metabolism and Its Sensitivity to Temperature. *J. Exp. Bot.* **2012**, *63*, 489–502. [CrossRef] [PubMed]
42. Siedliska, A.; Baranowski, P.; Pastuszka-Woźniak, J.; Zubik, M.; Krzyszczak, J. Identification of Plant Leaf Phosphorus Content at Different Growth Stages Based on Hyperspectral Reflectance. *BMC Plant Biol.* **2021**, *21*, 28. [CrossRef] [PubMed]
43. Yu, M.; Zeng, J.; Li, Y.; Fan, W.; Wang, L.; Wang, H.; Bao, J. Near-Infrared Prediction of Total Phosphorus in Leaves Content in Korla Fragrant Pear with Growth Period Specificity via Spectral Modeling. *Front. Plant Sci.* **2025**, *16*, 1666460. [CrossRef] [PubMed]
44. Wang, M.; Zheng, Q.; Shen, Q.; Guo, S. The Critical Role of Potassium in Plant Stress Response. *Int. J. Mol. Sci.* **2013**, *14*, 7370–7390. [CrossRef] [PubMed]
45. Jin, S.H.; Huang, J.Q.; Li, X.Q.; Zheng, B.S.; Wu, J.S.; Wang, Z.J.; Liu, G.H.; Chen, M. Effects of Potassium Supply on Limitations of Photosynthesis by Mesophyll Diffusion Conductance in Carya Cathayensis. *Tree Physiol.* **2011**, *31*, 1142–1151. [CrossRef] [PubMed]
46. Arnon, D.I. Dennis Robert Hoagland: 1884-1949. *Science* **1950**, *112*, 739–742. [CrossRef] [PubMed]
47. Conrad, O.; Bechtel, B.; Bock, M.; Dietrich, H.; Fischer, E.; Gerlitz, L.; Wehberg, J.; Wichmann, V.; Böhner, J. System for Automated Geoscientific Analyses (SAGA) v. 2.1.4. *Geosci. Model Dev.* **2015**, *8*, 1991–2007. [CrossRef]
48. Gitelson, A.A.; Kaufman, Y.J.; Merzlyak, M.N. Use of a Green Channel in Remote Sensing of Global Vegetation from EOS-MODIS. *Remote Sens. Environ.* **1996**, *58*, 289–298. [CrossRef]
49. Merzlyak, M.N.; Gitelson, A.A.; Chivkunova, O.B.; Rakitin, V.Y. Non-Destructive Optical Detection of Pigment Changes during Leaf Senescence and Fruit Ripening. *Physiol. Plant.* **1999**, *106*, 135–141. [CrossRef]
50. Gitelson, A.A. Wide Dynamic Range Vegetation Index for Remote Quantification of Biophysical Characteristics of Vegetation. *J. Plant Physiol.* **2004**, *161*, 165–173. [CrossRef] [PubMed]
51. Haboudane, D.; Miller, J.R.; Pattey, E.; Zarco-Tejada, P.J.; Strachan, I.B. Hyperspectral Vegetation Indices and Novel Algorithms for Predicting Green LAI of Crop Canopies: Modeling and Validation in the Context of Precision Agriculture. *Remote Sens. Environ.* **2004**, *90*, 337–352. [CrossRef]
52. Rondeaux, G.; Steven, M.; Baret, F. Optimization of Soil-Adjusted Vegetation Indices. *Remote Sens. Environ.* **1996**, *55*, 95–107. [CrossRef]
53. Daughtry, C.S.T.; Walthall, C.L.; Kim, M.S.; de Colstoun, E.B.; McMurtrey, J.E. Estimating Corn Leaf Chlorophyll Concentration from Leaf and Canopy Reflectance. *Remote Sens. Environ.* **2000**, *74*, 229–239. [CrossRef]
54. Haboudane, D.; Miller, J.R.; Tremblay, N.; Zarco-Tejada, P.J.; Dextraze, L. Integrated Narrow-Band Vegetation Indices for Prediction of Crop Chlorophyll Content for Application to Precision Agriculture. *Remote Sens. Environ.* **2002**, *81*, 416–426. [CrossRef]
55. Jordan, C.F. Derivation of Leaf-Area Index from Quality of Light on the Forest Floor. *Ecology* **1969**, *50*, 663–666. [CrossRef]
56. Qi, J.; Chehbouni, A.; Huete, A.R.; Kerr, Y.H.; Sorooshian, S. A Modified Soil Adjusted Vegetation Index. *Remote Sens. Environ.* **1994**, *48*, 119–126. [CrossRef]
57. Barnes, E.; Clarke, T.; Richards, S.; Colaizzi, P.; Haberland, J.; Kostrzewski, M.; Waller, P.; Choi, C.; Riley, E.; Thompson, T.; et al. Coincident detection of crop water stress, nitrogen status and canopy density using ground based multispectral data. In *Proceedings of the Fifth International Conference on Precision Agriculture, Bloomington, MN, USA, 16–19 July 2000*; American Society of Agronomy: Madison, WI, USA; Crop Science Society of America: Madison, WI, USA; Soil Science Society of America: Madison, WI, USA, 2000; Volume 1619, p. 6.
58. Fitzgerald, G.; Rodriguez, D.; O'Leary, G. Measuring and Predicting Canopy Nitrogen Nutrition in Wheat Using a Spectral Index—The Canopy Chlorophyll Content Index (CCCI). *Field Crops Res.* **2010**, *116*, 318–324. [CrossRef]
59. Bremner, J.M. Nitrogen-Total. In *Methods of Soil Analysis*; John Wiley & Sons, Ltd.: Hoboken, NJ, USA, 1996; pp. 1085–1121, ISBN 978-0-89118-866-7.
60. Olsen, S.R. *Estimation of Available Phosphorus in Soils by Extraction with Sodium Bicarbonate*; U.S. Department of Agriculture: Washington, DC, USA, 1954.
61. Pedregosa, F.; Varoquaux, G.; Gramfort, A.; Michel, V.; Thirion, B.; Grisel, O.; Blondel, M.; Prettenhofer, P.; Weiss, R.; Dubourg, V.; et al. Scikit-learn: Machine Learning in Python. *J. Mach. Learn. Res.* **2011**, *12*, 2825–2830.
62. Seabold, S.; Perktold, J. Statsmodels: Econometric and Statistical Modeling with Python. In Proceedings of the 9th Python in Science Conference, Austin, TX, USA, 28 June–3 July 2010; pp. 92–96.
63. Hunter, J.D. Matplotlib: A 2D Graphics Environment. *Comput. Sci. Eng.* **2007**, *9*, 90–95. [CrossRef]
64. The Jamovi Project. *Jamovi*, Version 2.6. Computer Software. The Jamovi Project: Sydney, Australia, 2025. Available online: https://www.jamovi.org (accessed on 15 May 2026).
65. Wu, Y.; Sun, M.; Zhao, Z.; Liang, Z.; Liu, J.; Liu, S. Uptake and Allocation of Newly Absorbed Nitrogen in Young Pear Trees Grafted onto Vigorous Rootstocks (*Pyrus betulifolia*). *Agronomy* **2022**, *12*, 2303. [CrossRef]

66. Jin, S.N.; Choi, D.G. Effects of different combinations of ammonium and nitrate nitrogen on growth, accumulation, and nitrate reductase activity in pear (*Pyrus pyrifolia* cv. Niitaka) seedlings. *Acta Hortic.* **2006**, *721*, 237–244.
67. Friedel, M.; Hendgen, M.; Stoll, M.; Löhnertz, O. Performance of reflectance indices and of a handheld device for estimating in-field the nitrogen status of grapevine leaves. *Aust. J. Grape Wine Res.* **2020**, *26*, 110–120. [CrossRef]
68. Bracke, J.; Elsen, A.; Adriaenssens, S.; Schoeters, L.; Vandendriessche, H.; Van Labeke, M.-C. Application of proximal optical sensors to fine-tune nitrogen fertilization: Opportunities for woody ornamentals. *Agronomy* **2019**, *9*, 408. [CrossRef]
69. Tremblay, N.; Wang, Z.; Bélec, C. Performance of Dualex in Spring Wheat for Crop Nitrogen Status Assessment, Yield Prediction and Estimation of Soil Nitrate Content. *J. Plant Nutr.* **2009**, *33*, 57–70. [CrossRef]
70. Goulas, Y.; Cerovic, Z.G.; Cartelat, A.; Moya, I. Dualex: A New Instrument for Field Measurements of Epidermal Ultraviolet Absorbance by Chlorophyll Fluorescence. *Appl. Opt.* **2004**, *43*, 4488–4496. [CrossRef] [PubMed]
71. Jarrell, W.M.; Beverly, R.B. The Dilution Effect in Plant Nutrition Studies. *Adv. Agron.* **1981**, *34*, 197–224. [CrossRef]
72. Haboudane, D.; Tremblay, N.; Miller, J.R.; Vigneault, P. Remote Estimation of Crop Chlorophyll Content Using Spectral Indices Derived From Hyperspectral Data. *IEEE Trans. Geosci. Remote Sens.* **2008**, *46*, 423–437. [CrossRef]
73. Barnes, J.D. Use of Nondestructive Spectroscopy to Assess Chlorophyll and Nitrogen in Fresh Leaves. Ph.D. Thesis, Utah State University, Logan, UT, USA, 1988.
74. Steyn, W.J.; Wand, S.J.E.; Holcroft, D.M.; Jacobs, G. Anthocyanins in Vegetative Tissues: A Proposed Unified Function in Photoprotection. *New Phytol.* **2002**, *155*, 349–361. [CrossRef] [PubMed]
75. Landi, M.; Tattini, M.; Gould, K.S. Multiple Functional Roles of Anthocyanins in Plant-Environment Interactions. *Environ. Exp. Bot.* **2015**, *119*, 4–17. [CrossRef]
76. Cartelat, A.; Cerovic, Z.G.; Goulas, Y.; Meyer, S.; Lelarge, C.; Prioul, J.L.; Barbottin, A.; Jeuffroy, M.-H.; Gate, P.; Agati, G.; et al. Optically Assessed Contents of Leaf Polyphenolics and Chlorophyll as Indicators of Nitrogen Deficiency in Wheat (*Triticum aestivum* L.). *Field Crops Res.* **2005**, *91*, 35–49. [CrossRef]
77. Meyer, S.; Cerovic, Z.G.; Goulas, Y.; Montpied, P.; Demotes-Mainard, S.; Bidel, L.P.R.; Moya, I.; Dreyer, E. Relationships between Optically Assessed Polyphenols and Chlorophyll Contents, and Leaf Mass per Area Ratio in Woody Plants: A Signature of the Carbon–Nitrogen Balance within Leaves? *Plant Cell Environ.* **2006**, *29*, 1338–1348. [CrossRef] [PubMed]
78. Cerovic, Z.G.; Masdoumier, G.; Ghozlen, N.B.; Latouche, G. A New Optical Leaf-Clip Meter for Simultaneous Non-Destructive Assessment of Leaf Chlorophyll and Epidermal Flavonoids. *Physiol. Plant.* **2012**, *146*, 251–260. [CrossRef] [PubMed]
79. Monje, O.A.; Bugbee, B. Inherent Limitations of Nondestructive Chlorophyll Meters: A Comparison of Two Types of Meters. *HortScience* **1992**, *27*, 69–71. [CrossRef]
80. Tremblay, N.; Wang, Z.; Cerovic, Z.G. Sensing Crop Nitrogen Status with Fluorescence Indicators. A Review. *Agron. Sustain. Dev.* **2012**, *32*, 451–464. [CrossRef]
81. Parkhill, J.P.; Maillet, G.; Cullen, J.J. Fluorescence-Based Maximal Quantum Yield for Psii as a Diagnostic of Nutrient Stress. *J. Phycol.* **2001**, *37*, 517–529. [CrossRef]
82. Dourado, P.R.M.; Paulino, M.K.S.S.; Leal, L.Y.d.C.; Araújo, C.A.F.; Nunes, J.A.; Oliveira, E.C.d.; Júnior, J.A.S.; Santos, A.d.C.; Leitão, D.A.H.d.S.; Nunes, M.R.; et al. Water Demand and Photosynthetic Performance of Tomatoes Grown Hydroponically Under Increasing Nitrogen Concentrations. *Water* **2025**, *17*, 1951. [CrossRef]
83. Kokaly, R.F.; Asner, G.P.; Ollinger, S.V.; Martin, M.E.; Wessman, C.A. Characterizing Canopy Biochemistry from Imaging Spectroscopy and Its Application to Ecosystem Studies. *Remote Sens. Environ.* **2009**, *113*, S78–S91. [CrossRef]
84. Watt, M.S.; Pearse, G.D.; Dash, J.P.; Melia, N.; Leonardo, E.M.C. Application of Remote Sensing Technologies to Identify Impacts of Nutritional Deficiencies on Forests. *ISPRS J. Photogramm. Remote Sens.* **2019**, *149*, 226–241. [CrossRef]
85. Thomson, E. Optical Remote Sensing of Vegetation Canopy Properties from Local to Global Scales. Ph.D. Thesis, University of Oxford, Oxford, UK, 2021.
86. Mediavilla, S.; Escudero, A. Relative Growth Rate of Leaf Biomass and Leaf Nitrogen Content in Several Mediterranean Woody Species. *Plant Ecol.* **2003**, *168*, 321–332. [CrossRef]
87. Koyama, L.; Tokuchi, N.; Fukushima, K.; Terai, M.; Yamamoto, Y. Seasonal Changes in Nitrate Use by Three Woody Species: The Importance of the Leaf-Expansion Period. *Trees* **2008**, *22*, 851–859. [CrossRef]
88. Yang, H.Q.; Lv, G. Determination of Pear Leaf Nitrogen Content Based on Multi-Spectral Imaging Technology and Multivariate Calibration. *Key Eng. Mater.* **2011**, *467–469*, 718–724. [CrossRef]
89. Wang, Z.; Wang, T.; Darvishzadeh, R.; Skidmore, A.K.; Jones, S.; Suarez, L.; Woodgate, W.; Heiden, U.; Heurich, M.; Hearne, J. Vegetation Indices for Mapping Canopy Foliar Nitrogen in a Mixed Temperate Forest. *Remote Sens.* **2016**, *8*, 491. [CrossRef]
90. Pandey, P.; Singh, S.; Khan, M.S.; Semwal, M. Non-Invasive Estimation of Foliar Nitrogen Concentration Using Spectral Characteristics of Menthol Mint (*Mentha arvensis* L.). *Front. Plant Sci.* **2022**, *13*, 680282. [CrossRef] [PubMed]
91. Carella, A.; Massenti, R.; Marra, F.P.; Catania, P.; Roma, E.; Lo Bianco, R. Combining Proximal and Remote Sensing to Assess 'Calatina' Olive Water Status. *Front. Plant Sci.* **2024**, *15*, 1448656. [CrossRef] [PubMed]

92. Zhao, C.; Wang, J.; Huang, W.; Zhou, Q. Spectral Indices Sensitively Discriminating Wheat Genotypes of Different Canopy Architectures. *Precis. Agric.* **2010**, *11*, 557–567. [CrossRef]
93. Kiranmai, Y.; Potdar, M.P.; Biradar, D.P.; Kuligod, V.B.; Kanade, A.K.; Parmar, B.; Malunjkar, V. Moisture Stress Assessment in Rabi Maize through UAV-Mounted Multispectral Sensor. *Front. Environ. Sci.* **2025**, *13*, 1651422. [CrossRef]
94. Yan, N.; Qin, Y.; Wang, H.; Wang, Q.; Hu, F.; Wu, Y.; Zhang, X.; Li, X. The Inversion of SPAD Value in Pear Tree Leaves by Integrating Unmanned Aerial Vehicle Spectral Information and Textural Features. *Sensors* **2025**, *25*, 618. [CrossRef] [PubMed]
95. Roma, E.; Catania, P.; Vallone, M.; Orlando, S. Unmanned Aerial Vehicle and Proximal Sensing of Vegetation Indices in Olive Tree (*Olea europaea*). *J. Agric. Eng.* **2023**, *54*. [CrossRef]
96. Sun, Y.; Huang, K.; Yuan, Q.; Lei, X.; Lv, X. A Two-Stage Canopy Extraction Method Utilizing Multispectral Images to Enhance the Estimation of Canopy Nitrogen Content in Pear Orchards with Full Grass Cover. *Horticulturae* **2025**, *11*, 1419. [CrossRef]
97. Evans, J.R. Photosynthesis and Nitrogen Relationships in Leaves of C3 Plants. *Oecologia* **1989**, *78*, 9–19. [CrossRef] [PubMed]
98. Ercoli, L.; Mariotti, M.; Masoni, A.; Massantini, F. Relationship between Nitrogen and Chlorophyll Content and Spectral Properties in Maize Leaves. *Eur. J. Agron.* **1993**, *2*, 113–117. [CrossRef]
99. Padilla, F.M.; Teresa Peña-Fleitas, M.; Gallardo, M.; Thompson, R.B. Evaluation of Optical Sensor Measurements of Canopy Reflectance and of Leaf Flavonols and Chlorophyll Contents to Assess Crop Nitrogen Status of Muskmelon. *Eur. J. Agron.* **2014**, *58*, 39–52. [CrossRef]
100. Dong, R.; Miao, Y.; Wang, X.; Chen, Z.; Yuan, F.; Zhang, W.; Li, H. Estimating Plant Nitrogen Concentration of Maize Using a Leaf Fluorescence Sensor across Growth Stages. *Remote Sens.* **2020**, *12*, 1139. [CrossRef]
101. Shi, P.; Wang, Y.; Yin, C.; Fan, K.; Qian, Y.; Chen, G. Mitigating Saturation Effects in Rice Nitrogen Estimation Using Dualex Measurements and Machine Learning. *Front. Plant Sci.* **2024**, *15*, 1518272. [CrossRef] [PubMed]
102. Deng, B.; Li, Y.; Xu, D.; Ye, Q.; Liu, G. Nitrogen Availability Alters Flavonoid Accumulation in Cyclocarya Paliurus via the Effects on the Internal Carbon/Nitrogen Balance. *Sci. Rep.* **2019**, *9*, 2370. [CrossRef] [PubMed]
103. Kaniszewski, S.; Kowalski, A.; Dysko, J.; Agati, G. Application of a Combined Transmittance/Fluorescence Leaf Clip Sensor for the Nondestructive Determination of Nitrogen Status in White Cabbage Plants. *Sensors* **2021**, *21*, 482. [CrossRef] [PubMed]
104. Mirabdulbaghi, M. Leaf Nutrient Status of Some Grafted-Pear Rootstocks Influenced by Different Soil Types. *Span. J. Agric. Res.* **2020**, *18*, 22. [CrossRef]
105. Suriyagoda, L.D.B.; Ryan, M.H.; Gille, C.E.; Dayrell, R.L.C.; Finnegan, P.M.; Ranathunge, K.; Nicol, D.; Lambers, H. Phosphorus Fractions in Leaves. *New Phytol.* **2023**, *237*, 1122–1135. [CrossRef] [PubMed]
106. Tian, Y.; Du, E.; Tang, Y.; Xia, N. Distinct Seasonality of Nutrients in Twigs and Leaves of Temperate Trees. *Tree Physiol.* **2025**, *45*, tpaf014. [CrossRef] [PubMed]
107. Kvakić, M.; Tzagkarakis, G.; Pellerin, S.; Ciais, P.; Goll, D.; Mollier, A.; Ringeval, B. Carbon and Phosphorus Allocation in Annual Plants: An Optimal Functioning Approach. *Front. Plant Sci.* **2020**, *11*, 149. [CrossRef] [PubMed]
108. Zhang, N.; Wang, J.; Dong, C. Quantification of Nutrients Lost by Annual Pruning, Leaf Abscission, and Fruit Harvest in Four Pear Cultivars. *HortScience* **2026**, *61*, 29–35. [CrossRef]
109. Cockefair, E.A. The Role of Phosphorus in the Metabolism of Plants. *Am. J. Bot.* **1931**, *18*, 582–597. [CrossRef]
110. Raghothama, K.G. Phosphorus and Plant Nutrition: An Overview. In *Phosphorus: Agriculture and the Environment*; John Wiley & Sons, Ltd.: Hoboken, NJ, USA, 2005; pp. 353–378, ISBN 978-0-89118-269-6.
111. Foyer, C.; Spencer, C. The Relationship between Phosphate Status and Photosynthesis in Leaves. *Planta* **1986**, *167*, 369–375. [CrossRef] [PubMed]
112. Zhao, S.; Blum, J.A.; Ma, F.; Wang, Y.; Borejsza-Wysocka, E.; Ma, F.; Cheng, L.; Li, P. Anthocyanin Accumulation Provides Protection against High Light Stress While Reducing Photosynthesis in Apple Leaves. *Int. J. Mol. Sci.* **2022**, *23*, 12616. [CrossRef] [PubMed]
113. Naing, A.H.; Kim, C.K. Abiotic Stress-Induced Anthocyanins in Plants: Their Role in Tolerance to Abiotic Stresses. *Physiol. Plant.* **2021**, *172*, 1711–1723. [CrossRef] [PubMed]
114. Zhang, X.; Zhang, M.; Zhao, T.; Deng, B. Phosphate Availability Regulates Flavonoid Accumulation Associated with Photosynthetic Carbon Partitioning in Cyclocarya Paliurus. *Physiol. Plant.* **2021**, *173*, 1956–1966. [CrossRef] [PubMed]
115. Daryanavard, H.; Postiglione, A.E.; Mühlemann, J.K.; Muday, G.K. Flavonols Modulate Plant Development, Signaling, and Stress Responses. *Curr. Opin. Plant Biol.* **2023**, *72*, 102350. [CrossRef] [PubMed]
116. Arrobas, M.; Afonso, S.; Ferreira, I.; Moutinho-Pereira, J.; Correia, C.; Rodrigues, M. Liming and Application of Nitrogen, Phosphorus, Potassium, and Boron on a Young Plantation of Chestnut. *Turk. J. Agric. For.* **2017**, *41*, 441–451. [CrossRef]
117. Carstensen, A.; Herdean, A.; Schmidt, S.B.; Sharma, A.; Spetea, C.; Pribil, M.; Husted, S. The Impacts of Phosphorus Deficiency on the Photosynthetic Electron Transport Chain. *Plant Physiol.* **2018**, *177*, 271–284. [CrossRef] [PubMed]
118. Hernández, I.; Munné-Bosch, S. Linking Phosphorus Availability with Photo-Oxidative Stress in Plants. *J. Exp. Bot.* **2015**, *66*, 2889–2900. [CrossRef] [PubMed]

119. Yue, X.L.; Liu, X.F.; Fang, S.Z. Influence of Nitrogen and Phosphorus Additions on Parameters of Photosynthesis and Chlorophyll Fluorescence in Cyclocarya Paliurus Seedlings. *Photosynthetica* **2023**, *61*, 318–327. [CrossRef] [PubMed]
120. Arena, M.E.; Pastur, G.M.; Lencinas, M.V.; Soler, R.; Bustamante, G. Changes in the Leaf Nutrient and Pigment Contents of *Berberis microphylla* G. Forst. in Relation to Irradiance and Fertilization. *Heliyon* **2020**, *6*, e03264. [CrossRef] [PubMed]
121. Valenzuela, J.L.; Sanchez, A.; Romero, L. Influence of Nitrogen, Phosphorus, and Potassium Fertilization on Foliar Pigments in Muskmelon Plants. *Commun. Soil Sci. Plant Anal.* **1994**, *25*, 1595–1604. [CrossRef]
122. Zhang, Y.; Wang, T.; Li, Z.; Wang, T.; Cao, N. Based on machine learning algorithms for estimating leaf phosphorus concentration of rice using optimized spectral indices and continuous wavelet transform. *Front. Plant Sci.* **2023**, *14*, 1185915. [CrossRef] [PubMed]
123. Gracia-Romero, A.; Kefauver, S.C.; Vergara-Díaz, O.; Zaman-Allah, M.A.; Prasanna, B.M.; Cairns, J.E.; Araus, J.L. Comparative Performance of Ground vs. Aerially Assessed RGB and Multispectral Indices for Early-Growth Evaluation of Maize Performance under Phosphorus Fertilization. *Front. Plant Sci.* **2017**, *8*, 2004. [CrossRef] [PubMed]
124. Picado, E.F.; Romero, K.F.; Heenkenda, M.K. Mapping Spatial Variability of Sugarcane Foliar Nitrogen, Phosphorus, Potassium and Chlorophyll Concentrations Using Remote Sensing. *Geomatics* **2025**, *5*, 3. [CrossRef]
125. Oivukkamäki, J.; Atherton, J.; Xu, S.; Riikonen, A.; Zhang, C.; Hakala, T.; Honkavaara, E.; Porcar-Castell, A. Investigating Foliar Macro- and Micronutrient Variation with Chlorophyll Fluorescence and Reflectance Measurements at the Leaf and Canopy Scales in Potato. *Remote Sens.* **2023**, *15*, 2498. [CrossRef]
126. Sun, G.; Hu, T.; Chen, S.; Sun, J.; Zhang, J.; Ye, R.; Zhang, S.; Liu, J. Using UAV-Based Multispectral Remote Sensing Imagery Combined with DRIS Method to Diagnose Leaf Nitrogen Nutrition Status in a Fertigated Apple Orchard. *Precis. Agric.* **2023**, *24*, 2522–2548. [CrossRef]
127. Dbara, S.; Melaouhi, A.; Mars, M.; Ben Mimoun, M. Potassium Uptake Efficiency of Two Pear Cultivars and Leaf Concentration at Deficiency Symptoms Appears. *J. Plant Nutr.* **2019**, *42*, 1660–1667. [CrossRef]
128. Shen, C.; Shi, X.; Xie, C.; Li, Y.; Yang, H.; Mei, X.; Xu, Y.; Dong, C. The Change in Microstructure of Petioles and Peduncles and Transporter Gene Expression by Potassium Influences the Distribution of Nutrients and Sugars in Pear Leaves and Fruit. *J. Plant Physiol.* **2019**, *232*, 320–333. [CrossRef] [PubMed]
129. Kumar, A.R.; Kumar, N.; Kavino, M. Role of Potassium in Fruit Crops—A Review. *Agric. Rev.* **2006**, *27*, 284–291.
130. Koo, R.C.J. Potassium Nutrition of Tree Crops. In *The Role of Potassium in Agriculture*; John Wiley & Sons, Ltd.: Hoboken, NJ, USA, 1968; pp. 469–487, ISBN 978-0-89118-250-4.
131. Kuzin, A.; Solovchenko, A. Essential Role of Potassium in Apple and Its Implications for Management of Orchard Fertilization. *Plants* **2021**, *10*, 2624. [CrossRef] [PubMed]
132. Marschner, H. *Marschner's Mineral Nutrition of Higher Plants*; Academic Press: Cambridge, MA, USA, 2011; ISBN 978-0-12-384906-9.
133. Ibaraki, Y.; Murakami, J. Distribution of Chlorophyll Fluorescence Parameter Fv/Fm within Individual Plants under Various Stress Conditions. *Acta Hortic.* **2007**, *761*, 255–260. [CrossRef]
134. Johnson, R.; Vishwakarma, K.; Hossen, M.S.; Kumar, V.; Shackira, A.M.; Puthur, J.T.; Abdi, G.; Sarraf, M.; Hasanuzzaman, M. Potassium in Plants: Growth Regulation, Signaling, and Environmental Stress Tolerance. *Plant Physiol. Biochem.* **2022**, *172*, 56–69. [CrossRef] [PubMed]
135. Lu, J.; Eitel, J.U.H.; Engels, M.; Zhu, J.; Ma, Y.; Liao, F.; Zheng, H.; Wang, X.; Yao, X.; Cheng, T.; et al. Improving Unmanned Aerial Vehicle (UAV) Remote Sensing of Rice Plant Potassium Accumulation by Fusing Spectral and Textural Information. *Int. J. Appl. Earth Obs. Geoinf.* **2021**, *104*, 102592. [CrossRef]
136. Huang, Y.; Li, D.; Liu, X.; Ren, Z. Monitoring Canopy SPAD Based on UAV and Multispectral Imaging over Fruit Tree Growth Stages and Species. *Front. Plant Sci.* **2024**, *15*, 1435613. [CrossRef] [PubMed]
137. Yu, M.; Fan, W.; Zeng, J.; Li, Y.; Wang, L.; Wang, H.; Han, F.; Bao, J. Machine Learning-Assisted NIR Spectroscopy for Dynamic Monitoring of Leaf Potassium in Korla Fragrant Pear. *Agronomy* **2025**, *15*, 1672. [CrossRef]

Disclaimer/Publisher's Note: The statements, opinions and data contained in all publications are solely those of the individual author(s) and contributor(s) and not of MDPI and/or the editor(s). MDPI and/or the editor(s) disclaim responsibility for any injury to people or property resulting from any ideas, methods, instructions or products referred to in the content.